HUMAN CAPITAL
NATIONAL COHESION STRATEGY

INSTITUTE OF METALLURGY
AND MATERIALS SCIENCE
OF POLISH ACADEMY OF SCIENCES

EUROPEAN
SOCIAL FUND

Kazimierz Drabczyk
Piotr Panek

Silicon-based solar cells

Characteristics and production processes

Ogniwa słoneczne na bazie krzemu

Charakterystyka i procesy wytwarzania

Kraków 2012

Peer review by:
prof. dr hab. inż. Grażyna Frydrychowicz-Jstrzębska
dr inż. Filip Granek

ISBN 978-83-62098-07-1

Printed by: PRINTPAP Łódź, www.printpap.pl

The paper was created within the frames of the project:
"Dissemination of the Achievements of Polish and Global Photovoltaics in the Process of Education on University Level – 2nd Edition"

Table of contents:

Project

This paper was created within the frames of the project: **"Dissemination of the Achievements of Polish and Global Photovoltaics in the Process of Education on University Level – 2nd Edition".** The project was attended by the students of Polish technical colleges. The general aim of the project was a dissemination of the knowledge on the achievements of Polish and global photovoltaics in the process of higher education, as well as on the resulting benefits for the energy sector in Poland.

The Polish sector of renewable energy sources remains far behind those of other EU countries (Germany, France), as well as the world's other highly developed countries (Japan, the USA), who are developing this manner of energy production. This is because Poland lacks any legal regulations which would support the development of photovoltaics and the generally understood market of renewable energy sources. Another reason is the lack – or insufficiency – of the knowledge on photovoltaics in the educational programs, both at the primary and the higher level.

That is the case despite the international obligations accepted by the Polish Republic which state that, up to 2010, the energy coming from renewable sources should constitute 7,5% of the total gross electric energy consumption, whereas at present, this index is placed at the level of about 3%.

Only the properly trained and educated specialist staff from the branch of renewable energy sources will make it possible to face these challenges, which is to implement systems of renewable energy as alternatives for the energy produced from carbon combustion. The project has contributed to the solution of this problem by a popularization of the knowledge on photovoltaics as the key element in the sector of renewable energy sources.

The aim of the project was: a presentation of the current achievements of the Polish and global photovoltaics and a creation of a platform for exchanging opinions and experience between the leading scientists in this field, during the II National Photovoltaics Conference, as well as a dissemination of the knowledge on the achievements of the Polish and global photovoltaics and a popularization of the awareness of the importance of this issue and its implications for the Polish economy. This aim was realized through trainings, workshops and a contest with a prize – an apprenticeship at the Photovoltaics Laboratory at the Polish Academy of Sciences. The tasks implemented within the project drew the students' attention to the possibilities and perspectives created by the sector of renewable energy sources, thus combining the educational system with the needs of the labour market, as well

as creating connections between science and economy, which will serve the creation of the society and economy based on knowledge.

The classes taught within the project were divided into two types: theoretical lectures and practical laboratory workshops.

The following issues were discussed during the theoretical lectures:

- Photovoltaic solar cells.
- Quantitative and qualitative characteristics of solar energy.
- Photovoltaic effect in the p-n junction.
- Materials used in photovoltaics.
- Construction of a typical solar cell.
- Technologies applied in photovoltaic cell production.
- Photovoltaic cell parameters and their measurement methods.
- Achievements of the Polish science in the field of photovoltaic cells.
- Research project realized by the Photoviltaics Laboratory at the Polish Academy of Sciences.
- Future of photovoltaics in Poland and in the world.

The topics discussed during the practical classes were as follows:

- Chemical preparation of silicon plates.
- High-temperature p-n junction formation process.
- Edges etching (Elimination of electrical short circuit from the cell's edges.)
- Deposition of an antireflection layer.
- Deposition of the cell's metallic contacts by screen printing.
- Measurements of the current-voltage and spectral characteristics of the produced cells.

The classes were held twice a month during the 2010/2011 academic year. The total training-workshop cycle for one training group equaled 60 didactic hours. The number of participants in each semester was 20. In total, the trainings and workshops were attended by 60 persons.

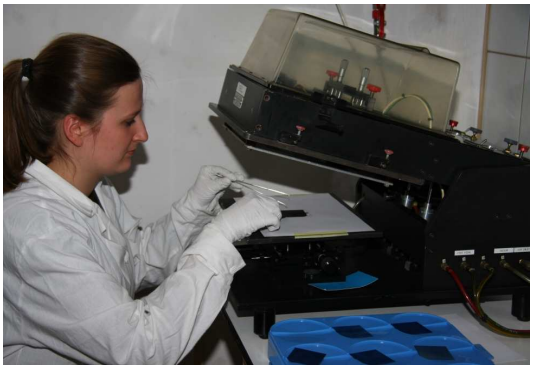


Students participating in the project during practical classes conducted at the Photovoltaics Laboratory at IMMS PAS.

The project also included the organization of the II National Photovoltaics Conference. It was attended by 70 participants representing 20 scientific and research centres, 9 commercial companies and 3 engineering and implementation institutions. The plenary sessions involved the discussion of the construction and operation of photovoltaic systems under the country's conditions, the aspects of the implementation of the system element production, as well as a presentation of exemplary photovoltaic products manufactured locally.

The subject matter of the conference sessions included the following issues:

- Crystalline and microcrystalline silicon-based solar cells – technology, properties and characteristics;
- Thin-layer solar cells with the CdTe, CIS and amorphous silicon basis;
- Solar cells with the organic compound basis;
- Measurements and characteristics of the material parameters and the solar cells' working parameters;
- Photovoltaic systems – working parameters and operation under local conditions,
- A session devoted to the specification of the research performed in cooperation with foreign centres,
- A session devoted to the industry's contacts with the research facilities in Poland (commercialization of the scientific test results),

A session devoted to the currently realized research projects at Polish scientific centers.

The project "Dissemination of the Achievements of Polish and Global Photovoltaics in the Process of Education on University Level – 2nd Edition" was financed by the Polish Government and the European Union within the European Social Fund.

1. Photovoltaics in the world – base materials and their producers

Photovoltaics (PV) is a scientific field which deals with obtaining electric energy from electromagnetic radiation energy, whose general and unlimited source is the Sun, and thus, single radiation-electric energy converters are called solar cells. The wide range of the world's photovoltaics is exhibited in the annual global, American, European and Asian conferences, where the most recent research and scientific achievements are verified among experts, and the parallelly held exhibitions present the newest developments made by the producers of materials, components, devices and measuring and diagnostic stations. For example, the XXVI European Photovoltaics Conference in 2011, in Hamburg (26th EU PVSEC in Hamburg, 999 exhibitors and 1,500 Conference presentations. Participants from more than 100 countries.), gathered over 4000 participants. The conference included presentations of 1500 lectures, and the parallelly held fair, during which about 999 exhibitors presented their products, was visited by about 41000 people from 103 countries. It can be stated that photovoltaics has become a new specialization in science and technology and, as an industrial sector, it now provides benefits not only in the form of a new type of unconventional method of electric energy production, but also in the stimulation of the economic and social development in those countries which see a big potential in its promotion.

Fig. 1. Exhibition halls and stalls of the companies from the PV sector presenting their products during the XXVI European Photovoltaic Conference, in 2011, in Hamburg.

The photovoltaic industry is a very modern and mostly automatized production sector, which applies advanced technologies and technical solutions. The efficiency of the production lines of a typical facility manufacturing 6-inch solar cells on the basis of crystalline silicon amounts to about 1500 items of solar cells per hour, which gives the annual production at the level of 50 MW_p. Solar cells are currently manufactured with the application of various methods and technological processes and with the use of numerous base materials, which are the most important discriminants of the five basic classification groups of the cells, presented in Fig. 2. Due to the existing number of types and diversified constructions of the cells, a lot of the latter's properties qualify them simultaneously to a few groups. Table 1 contains only a basic division of solar cells together with a specification of the cell types which are the most frequent representatives of the given group. The table also includes the values of photovoltaic conversion efficiency (E_{ff}), that is the ratio of the power obtained from the cell to the illumination power, for the best cells produced under laboratory conditions and for the typical photovoltaic modules, available as commercial market products. Table 1 does not include the efficiency of high-performance modules.

Tab. 1. Basic solar cell types classified according to groups and the highest photovoltaic conversion efficiencies for a given cell (E_{ff} of the cell), module (E_{ff} of the module), and the module producers of a given cell type [1], [2].

Cell group	Cell type	E_{ff} of cell [%]	E_{ff} of module [%]	Module producer
Crystalline Si	Mono-crystalline (Cz-Si)	24,7	22,7	SunPower – USA [3]
	Poly-crystalline (mc-Si)	20,3	18,6	Mitsubishi – Japan [4]
	Micro-crystalline (µc-Si)	11,7	10,9	Sanyo - Japan [1]
	Ribbon (R-Si)	-	13,4	Evergreen - USA [5]
	HIT	21,8	17,3	Sanyo – Japan [2]
High-performance	GaAs	25,8	-	-
	InP	21,9	-	-
	$GaInP_2/GaAs$	39,3	-	-
Thin-layer	CdTe	16,5	10,1	First Solar – USA [2]
	CIGS	19,5	12,2	Solibro - Germany [1]
	Amorphous Si (a-Si)	10,1	7,5	NES - China [6]
Organic	Polymer	5,1	1,8	Konarka - USA [6]
Photochemical	Dye – Grätzel	11,4	11,1	Sharp - Japan [3]

As it can be concluded from the comparative analysis of the photovoltaic conversion efficiency E_{ff} of cells and PV modules, the efficiency of the latter is always lower than that of the cells, due to the proportion of the total surface of the cells to the surface of the module, which is always lower than unity, and also, due to the slight reflection of light from the glass panels which protect the module and which are simultaneously its carrying material, as well as from the foils hermetizing the cells in the module.

.

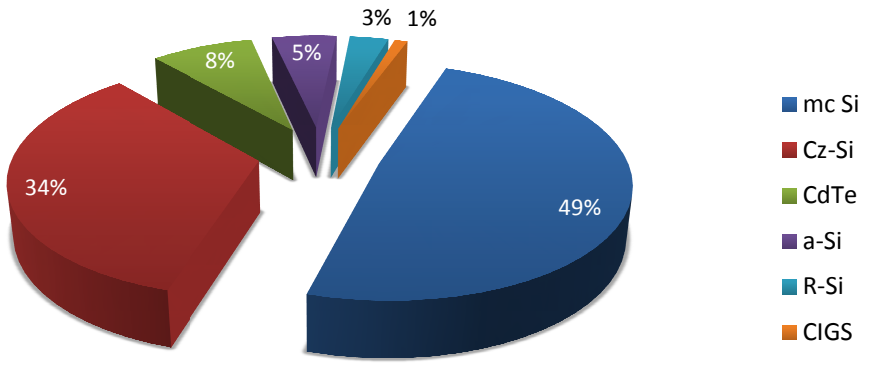

Fig. 2. Proportional share of a given solar cell type in the total solar cell production of global photovoltaics in 2008 [2].

The comparison of the proportional share of particular types of solar cells manufactured in 2008 unequivocally points to the domination of the crystalline silicon-based cells and a significant share of the thin-layer cells type CdTe and CIGS. In 2009, the share of the thin-layer cells increased up to nearly 19 %, due to the increase in the CdTe cell production by the American company, First Solar. The issue necessary to resolve is the five-percent share of the a-Si amorphous silicon-based cells. This value partially refers to the HIT –type cells produced by the Japanese company, Sanyo, whose base material is mono-crystalline silicon, and the emitter is formed by an amorphous silicon layer.

The domination of the Cz-Si and mc-Si cells results from several facts, which can be presented in the following points:

- A very good knowledge of the material and a developed research and diagnostic, Si-oriented, base, also resulting from the previous achievements of the electronic industry.

- An existing production capacity and a perfect mastering of the Czochlarski method (Cz-Si), as well as the casting method of the base material production, as well as unlimited resources of the charge raw material, SiO_2.
- An elaboration of a technological process allowing for a nearly automatic production of solar cells, with the average single cell surface equaling 236 cm^2.
- Already installed production capacities for cells and modules, in factories with a typical efficiency in the range of 50 ÷ 100 MW_p per year, together with a developed network of machine and material suppliers.
- Time-wise stability of the work parameters of cells and modules, allowing the producers to grant a 25-year warranty
- The amount of the financial capital invested in the last ten years.

According to the long-term forecasting, the crystalline silicon-based solar cells, including the ribbon and HIT silicon cells, will maintain their leading position in the volume of global production, with a simultaneous increasing share of the thin-layer cells, type CIGS and CdTe, up to about 20 %. The above mentioned cell types, as the most important and basic component elements of photovoltaic systems, are the only ones seriously considered by the industrial producers, who are the motor of a dynamic development of photovoltaics as an economical sector, whose income amounted to as much as 38,5 mld dollars in 2009 [7]. The dynamics of this growth is best reflected by a graphic compilation of the evolution of the global annual installations and the evolution of the global cumulative installed capacity 2000 – 2011 (MW), which is presented in Fig. 3. The included values prove a continuous dynamics of the PV sector's development and at the same time, show that photovoltaics is becoming a reckoned form of unconventional power engineering. According to EPIA (European Photovoltaic Industry Association), PV is, at present, after hydro and wind power, the third most important renewable energy source in terms of the globally installed capacity [8].

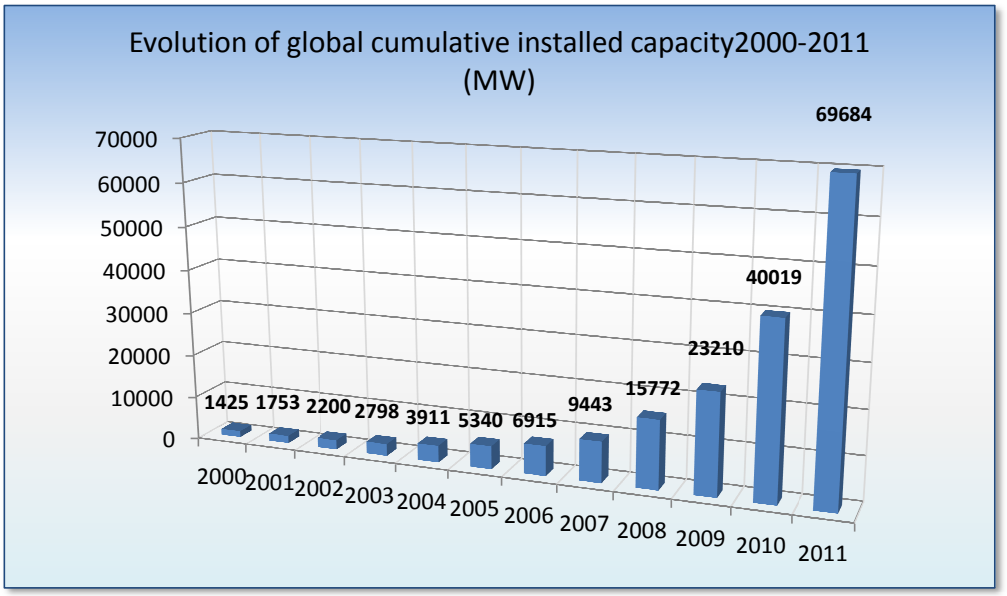

Fig. 3. Total capacity of all types of solar cells globally manufactured in particular years [7], [8].

The global photovoltaic industry, starting from the producers of solar cell base materials, through the manufacturers of cells, modules, device and material suppliers, up to the companies specializing in photovoltaic system installation, currently amount to 11000 enterprises. In China alone, there are, at present, 100 companies specializing in silicon production, about 100 companies producing solar cells and nearly 500 companies dealing with the manufacture of photovoltaic modules. The producers of thin-layer cells and modules amount to nearly 50 enterprises. In Taiwan, 26 companies deal with the cell production, 32 companies assemble modules and 19 companies produce thin-layer cells and modules. In comparison to the Far East economies, Europe remains clearly behind, and only the German PV sector provides a reckoned position in this field. In Europe, solar cells are produced only by 37 companies, modules – by 113 companies, and the production of thin-layer cells and modules is localized in 31 enterprises [9]. Analyzing also the investment scale in the PV sector, one can state that the biggest solar cell producers have their factories localized in China and Taiwan, which makes the proportional share of all the produced solar cells in 2009 amount to 49% only in those two countries.

Tab. 2. Biggest global producers of crystalline silicon-based solar cells and their existing production potential in 2009 [10].

Company	Country	Capacity [MW_p]
Suntech Power	Chiny	1000
Q-cell	Niemcy	910
JA Solar	Chiny	600
Tianwei Yingli SC	Chiny	600
Motech Industustries	Taiwan	580
SunPower	USA	574
CSI Canadian Solar	Chiny	570
Gimtech Energy	Taiwan	560
Trina Solar	Chiny	550
Sharp Corporation	Japonia	550

Tab. 3. Biggest global producers of crystalline silicon-based solar modules and their existing production potential in 2009 [10].

Company	Country	Capacity [MW_p]
Suntech Power	Chiny	1400
Best Solar	Chiny	800
Canadian Solar Technologies	Kanada	800
Baoding Tianwei Yingli Solar	Chiny	600
SunPower	USA	574
Trina Solar	Chiny	550
Sharp Corporation	Japonia	550
SolarFun Power	Chiny	480
Solon SE	Niemcy	460
SolardWorld AG	Niemcy	450

As can be concluded from the compilation provided by Tables 2 and 3, the dominating position in the PV market belongs to such countries as: China, Germany, the USA, Japan and Taiwan. This group will be probably soon extended by India, where the development of photovoltaic is extremely dynamic, although based on medium-size cell and module producers. China, Germany and the USA are also the biggest producers of the most important base material for the production of solar cells, which is crystalline silicon.

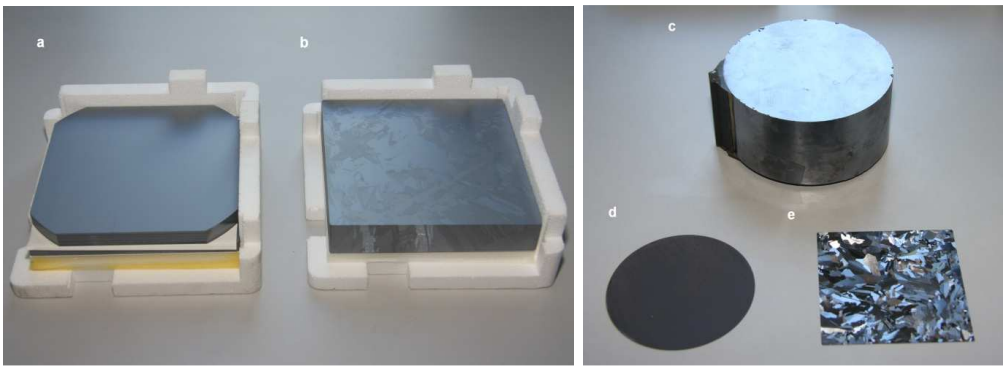

Fig. 4. Provided by the producer, original pack of 125 items of six-inch mono-crystalline silicon wafers Cz-Si (a) and poly-crystalline silicon plates mc-Si (b), 200 µm thick, used in the solar cell production. Fragment of a silicon Cz-Si roller made with the Czochralski process (c) and the cut-out plate used in the IC *(Integrated Circuit) sector* (d), next to a four-inch single mc-Si silicon plate, after the elimination of the defected layer, resulting from the block sawing (e).

Tab. 4. Value of the global production of crystalline silicon for electronics (sector IC) and photovoltaics (sector PV) up to 2008, and the forecast value for the years 2009 and 2010, as well as the average mass value of a crystalline silicon plate, used in the production of 1 Watt of a solar cell capacity – SSC [10].

Year	Si Production [tonne/year]		SSC [g/W_p]	Cell production [MW_p]
	Sector IC	Sector PV		
2004	18500	14300	13	1100
2005	19500	16300	11	1800
2006	20400	18850	10	2400
2007	21400	29300	9.0	4100
2008	22500	67500	8.5	6900
2009	23600	86250	8.0	9300
2010	24700	97800	7.5	13000

The development of the PV sector is connected with the significant growth of the crystalline silicon production and the systematic drop of the SI cells' thickness, which at the beginning of the decade equaled 300 µm, and now has been reduced to 200 µm, although there are already producers who offer 175 µm thick cells. A further thickness reduction, down to the level of 100 ÷ 120 µm, is also possible with the use of new construction concepts for the cells with the back contact points made by means of a laser radiation beam, type LFC *(Laser Fired Contact)*, the cells with MWT *(Metallization Wrap Through) or the cells with* IBC *(Interdigitated Back Contact).* In order to obtain a crystalline silicon plate, ready for the cell production, it is necessary to apply numerous processes, whose implementation is basically possible

only for the big producers, as the construction cost of such a facility is estimated by the American experts to amount to a minimum of 250 mln dollars. The PV sector involves the production of polycrystalline silicon (mc-Si) type p by means of casting, which is often called the multicrystalline silicon due to the big sections of its grains – of the order of 3 ÷ 20 – as well as mono-crystalline silicon (Cz-Si) of a lower quality, that is one with a higher level of impurities and defects of the crystal lattice. Crystalline silicon used in photovoltaics is referred to as the SG (*Solar Grade*) silicon and its quality is lower than that which is used in electronics and which is designated as the EG (*Electronic Grade*) silicon, in which an exemplary value of carbon equals 0,1 ppm ($5x10^{15}$ atoms/cm^3) and the oxygen content is 0,01 ppm. Fig. 5 schematically presents the process of obtaining crystalline silicon for electronics and photovoltaics.

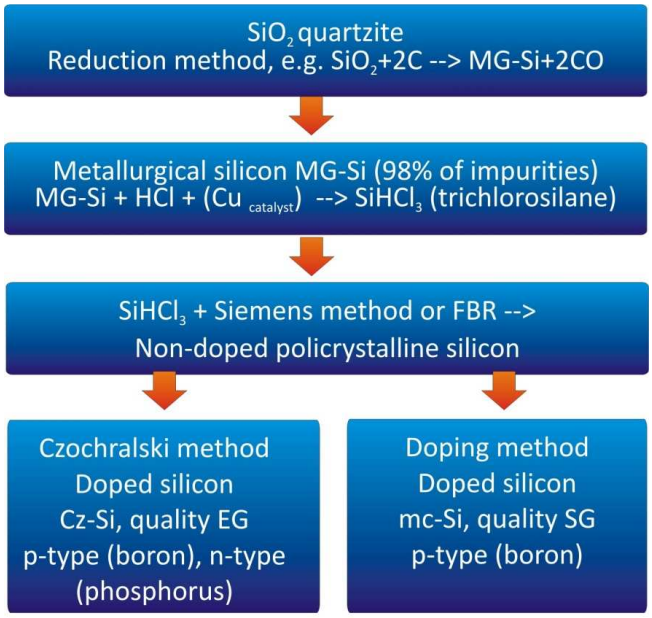

Fig. 5. Scheme of the production process of crystalline silicon for the IC and PV sectors.

Three of the biggest producers of non-doped polycrystalline silicon, which are Hemlock (USA), Wacker (Germany) i Tokuyama (Japan), apply the Siemens method, in which polycrystalline silicon, 20 cm in diameter, is created in a trichlorosilane reactor, on a crystalline silicon bar, 10 mm in diameter, heated up to 1100 ^{o}C. This process takes a few days and requires the provision of 200 kWh electric energy in order to obtain 1 kg of silicon. In an alternative method, FBR *(Fluidised Bad Reactor), the polycrystals of silicon are created in the form of granulate, in a continuous process* with $SiHCl_3$ at the temperature of 1000 ^{o}C, or SiH4 at the temperature of 700 ^{o}C [2].

The method which allows for a further purification of the mc-Si silicon and the obtaining of mono-crystalline silicon is zone melting, in which the FZ (*Float Zone) silicon is* obtained. The basic method of the Si mono-crystal production for the electronic industry is the Czochralski method. It involves the crystallization of the melted Si on the rotating mono-crystal nucleus, and the formation of a big mono-crystal in the form of a roller, with the crystallographic orientation defined by that of the nucleus. The silicon for the PV sector is also manufactured through the stretching of Si from the melted material out to the form of a ribbon (R-Si), which is created on a graphite matrix (the EFG *(Edge-defined Film-fed Growth) silicon) or between strained strings* (the SR *(String Ribbon) silicon). This method is used in practice by the American company,* Ever Green. Similar results can be obtained through the method of deposition on molybdenum or graphite bases (the RGS (*Ribbon Growth on Substrate*) silicon) or ceramic bases (the SOC (*Silicon on Ceramic*) silicon) [11]. There is a number of other methods of crystalline silicon production for photovoltaics, such as the recrystallization of Si powder by means of laser or the crystallization of amorphous silicon through the reaction with the aluminium layer, but basically, those reckoned in the mass production of solar cells based on Si type p are: the polycrystalline mc-Si silicon manufactured through directional crystallization, in the process of casting, in blocks of a typical weight of 450 kg; the mono-crystalline Cz-Si silicon, manufactured with the Czochralski method; and, partially, the ribbon R-Si silicon. In the last range, one can observe a certain increase in the interest in the Cz-Si silicon type n, which gives the possibility to produce solar cells with the E_{ff} value above 24 % [12]. The increase in the degree of silicon utilization is also stimulated by the improvement in the process of cutting blocks into single plates, with the use of diamond wire saws. Due to the technology development, the presently applied 200 micrometer wire diameters are being replaced by 150 – 120 µm ones, and this directly effects the increase in the number of the plates obtained from one block of crystalline silicon. The technological advancement in the production processes of the photovoltaic sector requires large financial inputs. An exemplary cost of an SG mc-Si silicon factory, with the capacity of about 3000 tons per year, allowing for the production of solar cells of the power of 275 MW_p per year, constructed by the Wacker Schott Solar company, in Jena, Germany, will amount to over 300 mln Euro. The mc-Si silicon factory, with the annual production capacity of 8000 tones, constructed in Taiwan by Formosa Chemicals & Fibre Corporation, will cost 1,03 billion USD [13]. The world's biggest silicon supplier, Hemlock, is planning an investment of the order of 4 billion USD, which, in 2014, will make it possible to increase the production from the current 30000 tons to 63000 tons per year [14].

2. Crystalline silicon cells

2.1 Photovoltaic effect – solar cell's current and voltage

The photovoltaic effect, which is the physical basis for the change of electromagnetic energy into electric one, consists in the creation of a non-compensated space electric charge in the given material medium, as a result of radiation absorption. The presence of this non-compensated charge results in the creation of electromotor force equaling the difference of potentials present at the terminals of the unloaded cell. If the cell terminals are closed with an outer circuit, then the conductor will be filled with direct current, its intensity being dependent on the value of the external resistance. In order for the cell to generate electric current, it is necessary to modify its structure by separating the positive and negative charge carriers in the conduction band. This separation occurs as a result of the carrier diffusion between the areas of different carrier concentrations, according to the electrochemical potential gradient, and also as a result of the charge convection in the internal electric field of the cell. An example of such a medium is the semiconductor crystalline silicon with a p-n junction. The formation of an area with the p-type conductivity takes place as a result of doping with atoms of acceptor elements for Si, from group III of the periodic system, whereas an area with the n-type conductivity is created as a result of doping with atoms of donor elements for Si, from group V of the periodic table. If the above structure of the crystalline Si material is exposed to radiation whose quantum energy is higher than its energy gap E_g = 1,12 eV, then a result of the light absorption is the generation of electric charge carrier pairs, electron-hole, which become separated under the effect of the electric field present in the junction. The consequence is an excess of electrons on the n-side and an excess of holes on the p-side, which results in the formation of electric voltage [15]. In a real solar cell made on the basis of crystalline silicon type p, the band structure, the potential distribution and the intensity of the electric field in the space charge of the p-n junction depend on the concentration of the donor impurity N_E and the acceptor impurity N_A. Figure 6 presents the band structure for an illuminated and non-illuminated solar cell, depending on the impurity concentration. The N_A impurity of the base material type p, homogeneous throughout the material, usually has the value of $1{,}5 \times 10^{16}$ atom/cm^3, which corresponds to the resistivity value of 1 Ωcm and it is usually obtained by boron doping. The N_E value is dependent on the impurity's profile and the concentration of the donor impurity N_D in the surficial area. Figure 6 schematically shows the effect of the formation of photovoltage V as a result of the cell's illumination. The calculations performed with the use of a PC-1D computer

software were realized with the assumption of the impurity profile type erfc for N_D = 3,6x10^{20} atom/cm^3 and the junction depth of 0,5 µm.

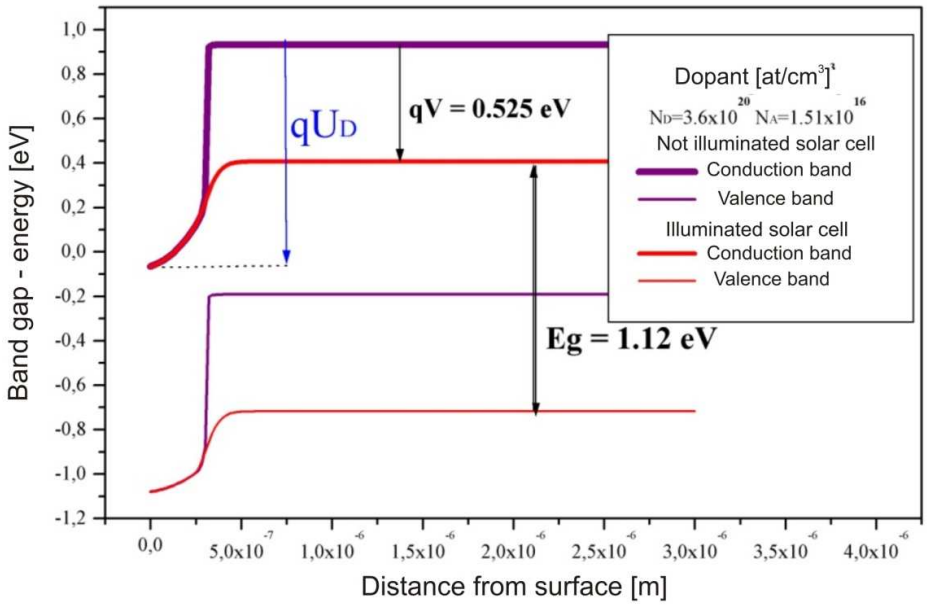

Fig. 6. Energy band displacement and creation of photovoltage V as a result of cell illumination, depending on the concentration of donor impurity N_D = 3,6x10^{20} atom/cm^3 and the homogeneous concentration of acceptor impurity N_A=1,5x10^{16} atom/cm^3.

As a result of the cell illumination, the position of the energy bans in the p-type area becomes lower by the value qV, which is mainly dependent on the acceptor impurity concentration. The value of the diffusion potential U_D depends on the impurity concentration according to the equation [16]:

$$U_D = kT/q \ln\left(N_A N_E / n_i^2\right) \qquad (1)$$

where: k - Boltzmann constant
T - temperature [^{o}K]
n_i - concentration of intrinsic charge carriers

The above dependences are highly significant for the design and production engineering of solar cells on the basis of crystalline silicon. If we lower the level of impurity N_A in the cell's base material, this will heighten its resistivity and the

consequence will be a decrease in the value of voltage at the cell's terminals. An increase of the N_A value causes, in turn, a decrease of the charge carriers' lifetime, mainly due to the process of Auger recombination, affecting the decrease in the intensity value of the current that is possible to be obtained from the cell. The cell current flowing in the external unloaded circuit which shorts the front and the back electrode will be a resultant of the photocurrent I_{ph} generated by the absorbed radiation reduced by dark currents I_1, I_2 and current I_r. The cell current I_{ph} will be originally the sum of the current generated in the space charge I_{SCR} and the current generated in the basis I_B. This is schematically illustrated in Figure 7, where the area of the space charge of width W is one which contains ionized donors and acceptors. The existence of electron currents in the cell is a symmetric reflection of the simultaneously occurring hole currents, with the basic difference of their size, resulting from the fact that the thickness of the emitter does not exceed 0.5 µm and the thickness of the base usually equals 200 µm. The photocurrent of the cell with the p-type silicon will thus originate mainly from the minor carriers, which, in the base, are constituted by the electrons.

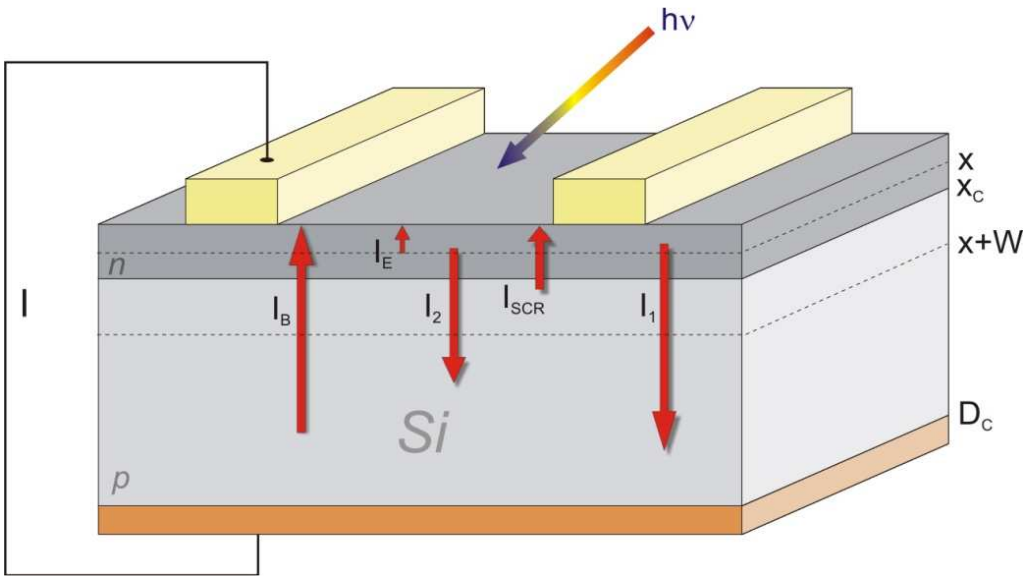

Fig. 7. Scheme of electron current component of a solar cell. W is the width of the space charge area and x_c is the depth of the p-n junction's position.

A detailed description of the origin of the current in the cell, schematically presented in Figure7, is contained in Table 5.

Tab. 5. Types of electron currents in a silicon solar cell.

No.	Current type	Symbol	Origin
1	Cell photocurrent	I_{ph}	Sum ($I_E + I_{SCR} + I_B$)
2	Emitter photocurrent	I_E	Electrons transferred from valence band to conduction band in n-type area
3	Space charge photocurrent	I_{SCR}	Electrons transferred from valence band to conduction band in space charge area
4	Base photocurrent	I_B	Electrons transferred from valence band to conduction band in p-type area
5	Dark diffusion current	I_1	Electrons penetrating beyond the potential's barrier from emitter to base
6	Dark diffusion-recombination current	I_2	Recombination of electron-hole pairs in space charge area Electrons tunneled from emitter's conduction band to base's valence band
7	Diffusion-recombination current of surface recombination	I_r	Electrons from conduction band in emitter's area recombining on cell's front surface

The total density of current J flowing through the p-n junction of surface area A_0 will thus be the sum of the density of the electron current J_e and the analogous density of the hole current J_h. If the density of all the dark currents, both the electron and the hole ones, is designated as J_0 , then, according to the Shockley equation [17]:

$$J = J_e + J_h = J_0\left[\exp\left(\frac{qV}{kT}\right) - 1\right] \qquad (2)$$

where :

$$J_0 = \frac{qD_h p_n}{L_h} + \frac{qD_e n_p}{L_e} \qquad (3)$$

In this dependence, the lower index (e) refers to the electrons and (h) refers to the holes. Symbols p_n and n_p designate the balance electron concentration in the n+tzpe material and the balance electron concentration in the p-type material, respectively. L is the diffusion length of the charge carriers, the electrons and the holes, connected with their lifetime τ by the following relation:

$$L = \sqrt{D\tau} \qquad (4)$$

where: D = μkT/q is the carrier diffusion coefficient of mobility μ.

If the electrodes of the cell are not short-circuited, then the result of the negative accumulation in the p area and the positive accumulation in the p will be an electric potential and the resulting photovoltage V, which lowers the energy barrier on the p-n junction. This causes a density increase of the dark currents up to the value compensating the density of the reverse current. This state corresponds to the highest value of the cell's photovoltage, which is called the open circuit voltage V_{oc} and which, according to (2), can be calculated from the following equation [17]:

$$V_{oc} = \frac{kT}{q} \ln\left(\frac{J}{J_0} + 1\right) \qquad (5)$$

With the assumption that all the impurity atoms are ionized and the value of the charge concentration in the equilibrium state in the semi-conductor equals $n_p N_A = p_n N_E$, we can prove that [16]:

$$\frac{d(V_{oc})}{dT} = \frac{1}{T}\left[V_{oc} - \frac{E_g}{q}\right] \qquad (6)$$

The formula describes the voltage change of the cells' open circuit with respect to temperature. The knowledge of this dependence is highly significant in the measurements of the cell's I-V characteristics and its practical exploitation. For example, for a Si cell, when V_{oc} equals 0,6 V, a temperature rise of one degree Celsius will cause a 1,7 mV drop of V_{oc}.

2.2 Reflection and absorption of electromagnetic radiation

For the radiation operating on the surface of the solar cell, it is necessary to minimize the reflection coefficient R_{ref} and the transmission coefficient T in such a way so as the total radiation can be absorbed within the volume of the cell's active material. The absorption coefficient $\alpha = 4\pi\nu\xi/c$ is equal to the inverse density x of that material's layer in which the radiation force P(0) of frequency ν decreases e times assuming the value P(x) according to the relation $P(x) = P(0)e^{-\alpha x}$. The quantity ξ is the extinction coefficient which is connected with the light refractive index n with the formula $n^* = n - i\xi$, where n^* designates the complex refractive index. In the case of oblique transitions, as is the case of silicon, α assumes the value $A(\nu)[h\nu - E_g \pm E_p]^2 / \{\pm\exp(\pm E_p/kT) - (\pm 1)\}$, where: E_p is the photon energy value, A(ν) is the function of energy and the reduced mass of the charge carriers and ± determines whether the photon is absorbed (+) or emitted (-) [18]. For the crystalline silicon, R_{ref} has the value of about 0,35 and thus its reduction is necessary. This is realized by coating the front surface of the cell with an antireflective layer (ARC) or by texturizing the cell's

surface, which results in the absorption of a part of the once reflected radiation. Proper texturization performed before the formation of the p-n junction makes it possible to expand the latter's surface and to improve the probability that the pairs of electrons and holes, which are generated in the area close to the junction, become separated [19]. In the case of the thin-layer cells, that is the cells of the density from a few to a few tens of micrometers, the texturization of the back surface makes it more probable that the unabsorbed radiation will reflect from the latter at the angle Φ being larger than the angle which satisfies the dependence given by Lambert: $\sin\Phi = 1/n^2$, describing the angle at which the photons reflected from the back surface leave the material of the light refractive index n and do not reflect from the front surface in the direction of the plate's inside. For Si the Lambert dependence gives the angle $\Phi = 17^o$. In order to precisely determine the effect of the ARC layer or the texture of the cell's surface on the reduction of the radiation reflection, photovoltaics introduces a quantity described as the effective reflection coefficient R_{eff}. It is defined by the following formula [20]:

$$R_{eff} = \int_{400}^{1100} R_{ref}(\lambda) N_{ph}(\lambda) d\lambda \; / \; \int_{400}^{1100} N_{ph}(\lambda) d\lambda \qquad (7)$$

where: $N_{ph}(\lambda)$ – the number of photons falling on a surface unit for a given wavelength per one second (solar spectrum in AM1.5).

The methods of surface texturization of crystalline silicon applied in the studies and production of solar cells are presented in Table 6. The value R_{eff} is given for the range 400 ÷ 1100 nm, which is the range of the wavelength of the radiation falling on the surface of the plate not coated with an additional ARC layer. For comparison, R_{eff} for the multicrystalline silicon, after block cutting, assumes the value of 34,8 % [21].

Some of the methods described in Table 6 are not suitable to be applied in production, due to their low efficiency, as in the case of method no.1,2 or 8, as well as some technological problems, such as the difficulty in creating a contact between the front electrode and the etched surfaces, which is the case of method no. 6. Method no. 7, which consists in chemical etching in KOH or NaOH solutions, is applied in industry for the texturization of Cz-Si silicon, with a crystallographic orientation of the surface (100), and method no.4, that is acid etching in HF-based solutions, is applied in the mass reduction of mc-Si cells. Research results also point to the possibility to use this method in removing the damaged layer from the surface of mc-Si plates, which are cut from blocks and whose surface is texturized [33].

Tab. 6. Methods of texturization of polycrystalline silicon surface applied in industry and research & development.

No.	TEXTURIZATION METHOD	R_{eff} [%]	TEXTURE TYPE
1	Etching in NaOH or KOH solutions with photolithographic masking	~20	Reversed regular pyramids [22]
2	Mechanical texturization with diamond saw	~5	Regular pyramids or grooves [23] [24]
3	Laser texturization	~10	Regular pyramids or grooves [25] [26]
4	Etching in HF-based acid solutions	~ 9	Sponge-type macro-porous layers [27]
5	Electrochemical anodization in HF solutions	~10	Macro-porous layers [28]
6	Plasma etching	~3	Irregular iglic-type pyramids [21] [29]
7	Etching in KOH and NaOH solutions without masking	~24	Regular and irregular geometric forms [30]
8	Etching in HNO_3-HF solutions with photolithographic masking	~3	Regular honeycomb-form texture [31] [32]
9	Etching in plasma with additional etching in KOH solution	~21	Irregular pyramids [21]

In high efficiency solar cells, the surface texturization is applied simultaneously with the ARC layer, which allows for a maximum reduction of R_{eff}. The ARC layer of the cell is required to fulfill a few basic conditions. One is to achieve the lowest possible value of the extinction coefficient ξ, which results in a high value of the transmission coefficient. As regards the value of the refractive index of the layer n_{arc}, it can be determined from the following relation:

$$n_{arc}d = \lambda_{opt}/4 \qquad (8)$$

where d is the thickness of the layer and λ_{opt} is the length of the wave for which the photon stream reaches its maximum [17]. Applying the Fresnel relation, one can calculate the minimum value of the reflection coefficient of the radiation operating from a medium of the light refractive index n_o, on the solar cell made of a material of the light refractive index n, coated with an ARC layer of the light refractive index n_{arc}. According to this dependence:

$$R_{ref} = \left(\frac{n_{arc}^2 - n_0 n}{n_{arc}^2 + n_0 n} \right)^2 \qquad (9)$$

Thus, the minimum value of R_{ref} equals zero for $n_{arc} = \sqrt{n_0 n}$. We determine the optimal parameters for the ARC layers applied in solar cells from relations (8) and (9). In the case of the silicon in which the refractive index n equals 3,87 for the wavelength of 632,8 nm, the optimal refractive index in the ARC layer equals 1,97 [34]. The refractive index in the typical materials used as ARC layers for silicon cells are presented in Table 7. With the aim of optimizing n_{arc}, especially for high efficiency cells, double layers are often applied, e.g. of the MgF_2/ZnS type. For a double ARC layer consisting of an upper and lower layer, whose refraction coefficients equal n_{1arc} and n_{2arc}, respectively, the reflection is minimal if the following condition is fulfilled [35]:

$$n_{2arc} = n^{1/2} \cdot n_{1arc} \qquad (10)$$

where $n_o < n_{1arc} < n_{2arc} < n$ and the particular layers fulfill the dependence (8).

Tab. 7. Light refractive index n_{arc} in materials applied as ARC layers in silicon solar cells.

No.	MATERIAL	COATING METHOD	n_{arc}
1	MgF_2/ZnS	Vaccuum coating	1,38 / 2,34 [34]
2	MgF_2/CeO_2	Vapour deposition/ion sputtering for target Ce	1,38 / 2,47[36]
3	SiO_2	Thermal oxidization	1,46 [34]
4	Si_3N_4	Gas phase deposition SiH_4:H_2:NH_3 in plasma	1,9 ÷ 2,3 [37] 1,9 ÷ 2,6 [34]
		High temperature gas phase deposition NH_3:$C_2H_6Cl_2Si$	1,55÷ 2,20 [38]
5	TiO_2	Hydrolysis with $Ti(OC_3H_7)_4$	2,38 ÷ 2,44 [39]
		Hydrolysis with $(C_2H_5O)_4Ti$	2,3 ÷ 2,5 [40]
6	$xSiO_2 \cdot yP_2O_5$	Gas phase deposition with $POCl_3$	1,71 ÷ 1,85 [41]
7	SnO_2	Hydrolysis with $SnCl_3 \cdot 5H_2O$	1,68 [42]
8	ZnO	Ion sputtering in atmosphere 1% O_2/Ar from target ZnO:Al_2O_3	1,9 ÷2,0 [43]

2.3 Series and parallel resistance of the cell

The parallel resistance R_{sh}, also called the shunt resistance, is connected with the resistance between the p-type silicon and the n-type silicon, in the area of the space charge. If, in this area, there are dislocations, grain boundaries or microfractures characteristic to the base material, or metallic bridges, formed during the diffusion process in the impure atmosphere or originated from the pastes after high

temperature contact metallization, then all these elements can be the ways for an easy leak of the already separated pairs of electrons and holes. This causes a drop in the photovoltage, especially for the multicrystalline silicon-based cells. A large drop of R_{sh} can take place on the edges of the cell, and this results from the easy access for outer metallic impurities. The series resistance is the sum of the resistances of particular components of the cell. According to Figure 8, this is the resistance of: the Si base material's contact, type p, to the rear contact R_1, the base material R_2, the Si emitter, type n, between the front electrodes R_3, the emitter's contact to the front electrode R_4 and the front electrode R_5. The resistance of the rear contact, made of a full metallic layer, should be considered as negligibly small. The resistance value of the contact R_4, which is fundamentally important for the efficiency of the cell and which depends on the paste type, the base resistance and the temperature of the metallization process, can be experimentally determined, e.g. with the use of the transmission line method [44]. For instance, for a cell with the surface area of 100 cm^2, characterizing in its fill factor value FF above 0,75 {the mentioned FF is discussed in Chapter 2.5, dependence (23)}, the value of R_s must be below 10 mΩ , and the value of R_{sh} – above 10 Ω.

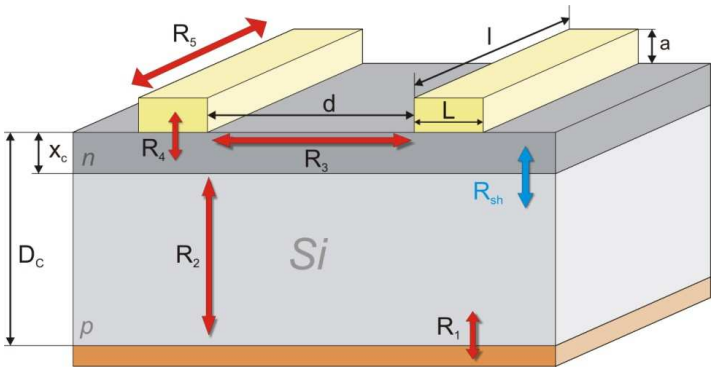

Fig. 8. Cross-section of a Si-based cell and the series resistance components.

Table 8 compiles the basic differences in the contact parameters of the front collecting electrode of a crystalline silicon-based solar cell, produced with the method of screen printing (SP), photolithography (PL) and chemical bath (CB), applied in BCSC cells with a buried contact (Chapter 2.6). The data refers to the resistivity value of the contact (R_4), which has a fundamental effect on the series resistance R_s of the cell, and also the resistivity value of the contact material, which affects R_5.

Tab. 8. Comparison of the effect of the basic production methods for collecting electrode contacts on the contact parameters and the fill factor FF of the cell [45]. The designations are in accordance with those in Figure 8.

Parameter	Contact forming method		
	Screen printing	Chemical bath	Photolithography
Height a	14 µm	50 µm	8 µm
Width L	80 µm	20 µm	20 µm
Contact resistivity	0.3 ÷ 3 mΩcm^2	3 µΩcm^2	0.01 mΩcm^2
Contact material resistivity	3 µΩcm	1.7 µΩcm	1.7 µΩcm
Fill factor FF	0,74 ÷ 0,77	0,78 ÷ 0,79	0,81 ÷ 0,82

2.4 Generation and recombination of charge carriers and quantum efficiency of the cell.

All the cell's volume, under the effect of the absorption of radiation with the photon energy E_{fot} larger than the energy gap E_g for Si, one can observe a generation of electron-hole pairs at the rate G(x), which increases the electron concentration in the conduction band and the hole concentration in the valence band. At the same time, the process of recombination takes place with the velocity $R_r(x)$, which causes some of the electrons to transit back to the valence band. Thus, the condition for the current to flow from the cell is the fulfillment of the following dependence:

$$G(x) - R_r(x) > 0 \qquad (11)$$

The generation rate G(x) is the function dependent on α and x according to the formula [17]:

$$G(x) = \int_0^{\infty} \alpha(\lambda) N_{ph}(\lambda)[1 - R_{ref}(\lambda)]\exp[-\alpha(\lambda)x]d\lambda \qquad (12)$$

The lifetime τ of the generated charge carriers, directly connected with the diffusion length by the dependence (4), in the silicon applied in photovoltaics, is of the order of a few tens of µs and, compared to the lifetime of the silicon with the highest electronic quality, which can even be over one millisecond, is very short. This results from the economical calculation, which takes into account the reduction of costs of the silicon production for sector PV, and this affects the flawing of the crystalline structure of Si and the level of impurities. The value τ is dependent on the carriers' lifetime as a result of the process of radiative recombination - τ_{rad}, the Auger

recombination - τ_{Auger} and trapping recombination - τ_{trap}, according to the formula [46]:

$$\frac{1}{\tau} = \frac{1}{\tau_{rad}} + \frac{1}{\tau_{Auger}} + \frac{1}{\tau_{trap}} \qquad (13)$$

For the impurity in Si which is lower than 10^{17} atom/cm^3 the radiative recombination is not significant. The trapping recombination is determined by the impurity level resulting from the technological process or the silicon quality, and generally, the lifetime of the carriers connected with its existence varies within the range of 10^{-3}-10^{-6} s. The determining factor for the carrier lifetime, in the case when the impurity concentration is above 10^{18} atom/cm^3, is the Auger recombination, which causes a linear drop of τ_{Auger} down to 10^{-10} s for the impurity concentration of 10^{20} atom/cm^3 [16]. The dependence of the charge carrier lifetime, or the proportional diffusion length from the impurity concentration to Si, is one of the basic issues in the thick-layered technology of crystalline silicon solar cell production. Silicon solar cells are produced on the basis of the p-type silicon with the acceptor impurity concentration N_A equaling 1,513 x 10^{16} atom/cm^3, which corresponds to the base material resistivity of 1 Ωcm. For the N_A value lower than the one given above, one can obtain a lower cell voltage V_{oc}, and for the N_A value of the order of 10^{17} atom/cm^3 and more, a drop of τ occurs, which is mainly caused by the Auger recombination, and this implies a drop of both I_{sc} and V_{oc}. The donor doped area of the n-type by the depth of about 0,4 μm is gradient in character, with the impurity concentration in the surface area of ~ 10^{22} atom/cm^3. The surface resistance R_ρ of this area, for a typical cell, is at the level of 40 ÷ 50 Ω/□, which does not cause problems in the creation of an ohm contact of a low resistivity ~ 3 mΩcm, between this area and the electrode. For the decreasing value of R_ρ the cell will have a lower I_{sc} value, and for R_ρ at the level of 60 ÷ 80 Ω/□ technological problems occur, which are connected with the proper metallization of the front electrode contact. This problem is often solved through such a construction of the selective emitter of the solar cell which contains an area whose R_ρ has the value of e.g. 30 Ω/□ directly under the front electrode paths, and an area with the R_ρ value of ~ 100 Ω/□ between these paths.

Solar cells differ from other electron devices in a much larger surface, which makes the latter's effect on the cell parameters highly significant. Breaking the crystal's periodicity on the surface and the existence of unsaturated bonds causes the appearance of additional acceptor energy levels localized in the silicon's energy gap. On the real Si surface, coated with a thin layer of natural oxide, one can find

acceptor, donor and trapping states. The effect of the surface on the kinetics of the electron processes is described by a quantity called surface recombination velocity S, defined as [47]:

$$S = \frac{J_r}{q \cdot \Delta n_e} = \sigma_r \upsilon_r N_r \qquad (14)$$

where: J_r – density of the electron or hole current flowing to the surface, for maintaining the established state in which the excess charge carrier concentration in the volume equals Δn_e,
N_r – number of recombination centres per surface unit,
σ_r – collision cross-section of charge carrier capturing,
υ_r – thermal velocity of charge carriers,

The surface recombination process taking place through defects is described by the Shockley-Read-Hall theory, according to which the recombination velocity increases with the increasing recombination centres N_r or free charge carrier concentration on the surface [48]. The increase of the surface recombination directly affects the increase of the current I_r, causing a drop of the voltage and the current possible to obtain from the cell [49]. That is why, on the surface of Si, thin layers of compounds are formed, whose atoms, combining with the surface semi-conductor atoms, complement their incomplete bondings, that is they passivize the surface. In practice, the surface passivation is realized through oxidization of the silicon plate surface in dry oxygen, at the temperature range of 800 ^{o}C ÷ 1100 ^{o}C. Another technique is coating the plate with a layer of hydrogenated silicon nitride with the method of plasma enhanced chemical vapour deposition (PECVD). The Si_xN_y:H layer, beside its passivating and protective effect on the Si-surface, is additionally advantageous in the fact that, during the high temperature metallization process of the front electrode, the hydrogen atoms released from the layer also passivize the material in its whole volume, which is a determining factor in the case of mc-Si cells [50]. The silicon nitride layer deposited by means of PECVD allows for a passivation of the Si surface, but at the same time, it plays the role of an antireflection coating. The Si_xN_y:H layer, due to its electron affinity, is appropriate for the n-type Si. In the case of the p-type Si surface, more suitable seems to be an Al_2O_3 layer, which is deposited with the method of ALD (Atomic Layer Deposition).

Tab. 9. Passivation coatings used in the silicon solar cell production and the surface recombination velocity (SRV) values obtained after applying the technology.

Layer type	Deposition method	SRV [cm/s]
SiO_2	Thermal	90 [51]
Si_xN_y:H	PECVD	10 [52]
Al_2O_3	ALD	70 [51]
a-Si:H	PECVD	30 [53]

The passivation coatings are especially important for the cells of the thickness below 200 µm. For the surface-polished silicon, SRV assumes values at the level of $10^5 \div 10^7$ cm/s. With the aim to evaluate the process of regeneration and recombination of the charge carriers in the surface layer, in the space charge layer and in the base, according to the character of light absorption of a given wavelength in Si, measurements of the quantum efficiency (QE) of the cell are performed. QE is defined as the ratio of the number of generated and separated electron-hole pairs to the number of photons of a given energy falling on the front side of the cell [54]. Two types of quantum efficiency are distinguished:

- External quantum efficiency (EQE), described by the following formula:

$$EQE(\lambda) = \frac{J(\lambda)}{qN_{ph}(\lambda)} \qquad (15)$$

where: J(λ) - density of the current from the solar cell for a given wavelength
$N_{ph}(\lambda)$ – number of the photons falling on the cell for a given wavelength per surface unit for the time of one $N_{ph}(\lambda)$ is expressed in $m^{-2}/$ s nm. It is connected with the radiation intensity P_{in} by the following dependence:

$$P_{in} = \int_{400}^{1100} N_{ph}(\lambda) h \frac{c}{\lambda} d\lambda \qquad (16)$$

- Internal quantum efficiency (IQE) – this takes into account only the radiation absorbed by the cell and is described by the following formula:

$$IQE(\lambda) = \frac{J(\lambda)}{qN_{ph}(\lambda)[1 - R_{ref}(\lambda)]} \qquad (17)$$

The knowledge of the quantum efficiency in a given range of radiation wavelength makes it possible to directly calculate the density of the short-circuit current of the cell from the formula (16) or (17), in the case when we know the reflection coefficient in this wavelength range, and it also allows for an evaluation of the efficiency of the photovoltaic process for a given cell area. An exemplary

dependence of the effect of the cell's rear contact engineering on the absorption and photogeneration of the charges in the longwave radiation range is presented in Figure 9.

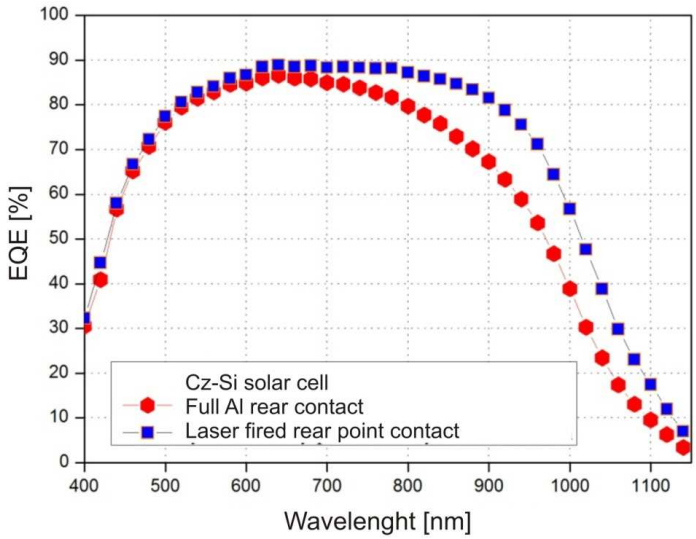

Fig. 9. External quantum efficiency of solar cells differing only in the construction and production technology of the rear contact.

2.5 Construction and production process of crystalline silicon solar cells

Silicon solar cells are constructed of a few basic elements which allow not only for a conversion of the electromagnetic radiation into direct current but also to lead the current to the outer circuit. Figure 10 shows a construction scheme of a classic silicon solar cell made in the screen process technology, produced by most of the global solar cell manufacturers.

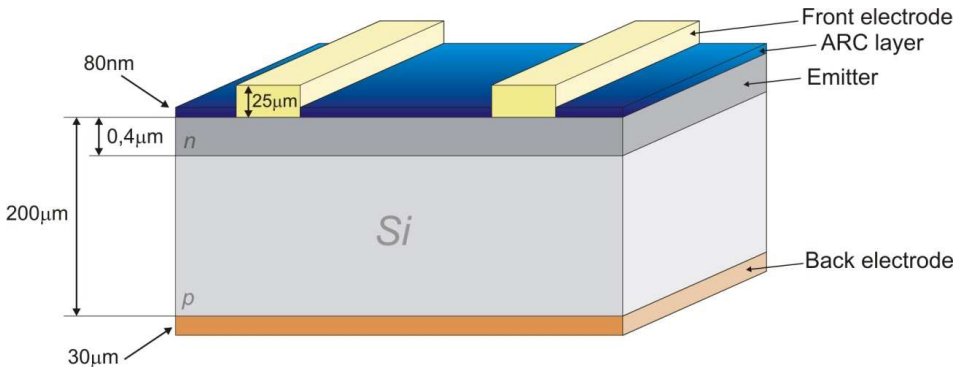

Fig. 10. Scheme of a solar cell with a given thickness value of particular construction elements.

Most of the global producers manufacture crystalline silicon solar cells with the technological process schematically presented in Figure 11. The applied base material are boron-doped monocrystalline silicon plates Cz-Si, type p, 200 μm thick, with the surface crystallographic orientation of (100), the resistivity of ~ 1 Ωcm and the charge carrier lifetime of τ ~ 20 μs. In the case of polycrystalline plates, the value of τ is usually lower, the crystallographic orientation is determined by the orientation of particular grains, and the remaining parameters are identical with those of the Cz-Si plates.

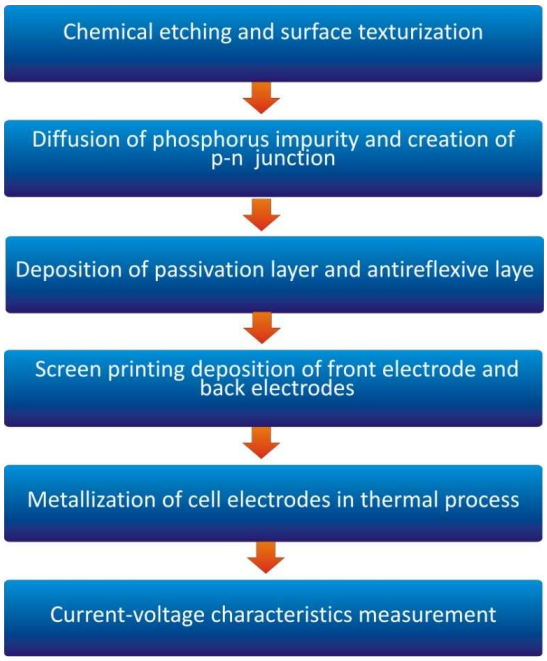

Fig. 11. Scheme of the technological process of silicon solar cell production.

I. Chemical etching and surface texturization

The mc-Si and Cz-Si silicon plates obtained from the producer have a defected surface, down to the depth of ~ 5 µm, formed as a result of diamond or wire saw cutting. The two-sided elimination of the defected layer is performed in the process of chemical etching in a KOH solution. In order to reduce the reflection coefficient R_{ref}, the surface of the plate is covered with texture. In the case of Cz-Si, the surface texturization is performed in the chemical process at the temperature of 80 ^{o}C for the time of 30 min. In a KOH:IPA:H_2O solution, the texturization of the mc-Si plates is conducted on the basis of the HF:HNO_3:H_2O acid solutions. In the next stage, which aims at the elimination of organic and metallic impurities, as well as natural oxides, the Si plates are placed in baths of H_2SO_4, HCl and HF solutions, respectively. Between each stage, the plates are rinsed in deionized water of resistivity not lower than 5 MΩcm. The reagents used in these processes must be in the chemical purity class of ”analytically pure”. Because of the applied types of chemical solutions, the plates are placed in teflon holders.

Fig. 12. Chemically prepared silicon pates placed in teflon holders (left) and chemical etching process (right).

The chemical processes performed before producing the p-n junction aim at the elimination the defected layer, a formation of a surface texture which reduces the coefficient of reflection from the silicon surface, as well as the cleaning of the surface of all impurities and oxides. Thus prepared Si wafer is placed in the reactor of a diffusion furnace.

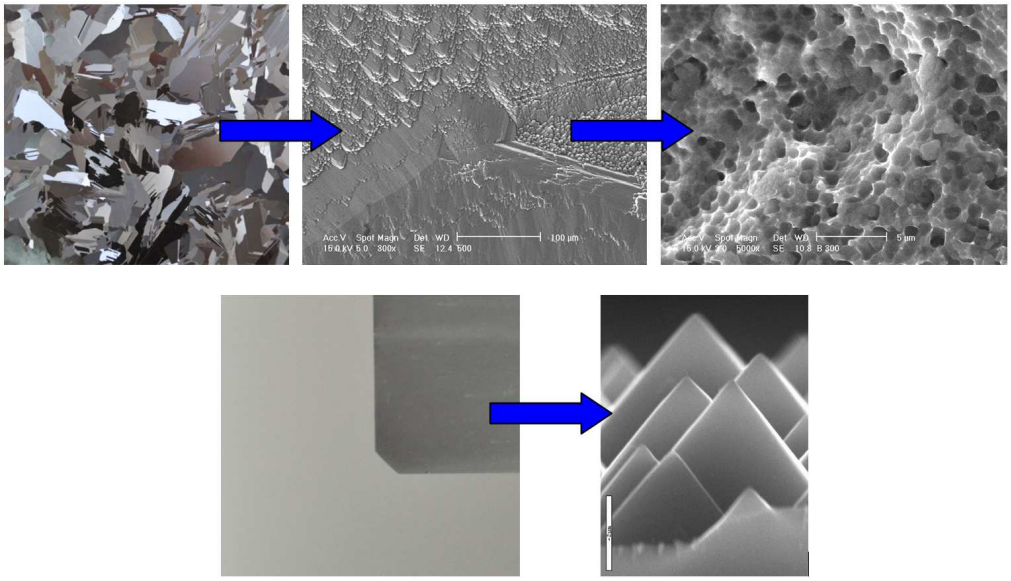

Fig. 13. Mc-Si silicon wafer, 25 cm^2 in surface area, after texturization in KOH solution, microphotograph of the area between grains, microphotograph of mc-Si after texturization in $HF:HNO_3:H_2O$, Cz-Si plate with crystallographic orientation (100) obtained from the producer, with a part of the surface texturized in KOH, microphotograph of texture (from left to bottom).

II. Diffusion of phosphorus impurity and p-n junction production

The p-n junction in the base silicon with the p-type conductivity is produced through diffusion of phosphorus atoms in the Si surface, the former originating from phosphorus oxychloride $POCl_3$. This is one of the most important stages of the cell production, determining the impurity concentration profile, which directly affects the process of generation and recombination of the charge carriers and the series resistance of the front electrode contact to silicon. The Si plates in the quartz holder are placed in a heated quartz reactor which is provided with protective gas N_2 and reactive gases $POCl_3$ and O_2. At the temperature above 800 ^oC, in the presence of oxygen, a dissolution of the $POCl_3$ occurs and, at the same time, phosphosilicate glass $xSiO_2 \cdot yP_2O_5$ (PSG) is formed on the Si surface, which further constitutes a local source of phosphorus diffusing in silicon. This process takes place according to the following dependences [55]:

$$4POCl_3 + 3O_2 \rightarrow 2P_2O_5 + 6Cl_2 \quad (18)$$

$$2P_2O_5 + 5Si \rightarrow 5SiO_2 + 4P \quad (19)$$

During diffusion, the doping atmosphere must be supplemented with oxygen, so that the partial pressure P_2O_5 is sufficient to saturate PSG with phosphorus atoms. As a result of the diffusion process, some of the impurity atoms do not assume the substitution sites in the crystalline silicon structure, but instead they assume the interstitial sites, thus forming an electrically inactive layer, the, so called, dead layer [56], [57].

Fig. 14. Industrial diffusion furnace (left) the plate holder entering the heated quartz reactor (right)

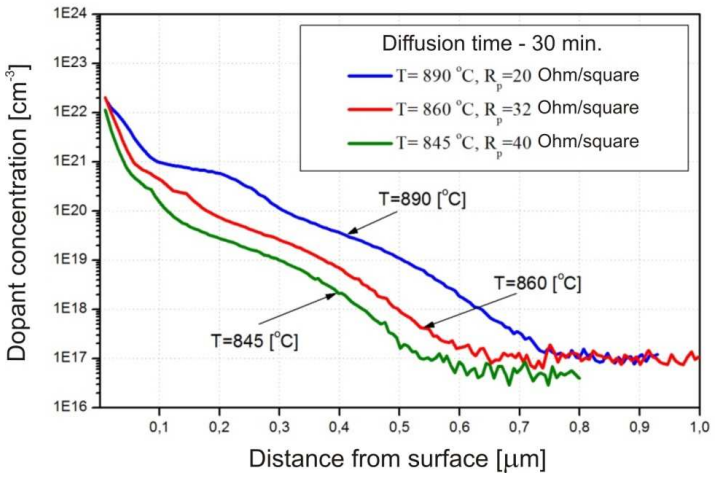

Fig. 15. Profiles of donor impurity distribution from source $POCl_3$ through secondary ion mass spectrometry (SIMS) at the Physics Institute PAN in Warszawa; together with the temperature value for the given diffusion process. The diagram also gives the surface resistance value R_ρ of the donor impurity layer.

The concentration and the profile of the impurity are affected by the temperature, time and concentration of the reactive gases. Following from the distributions of the n-type impurity, presented in Figure 15, the orientation of the junction for R_ρ = 40 Ω/□ is at the depth of about 0,6 µm from the plate surface, where

a change of the conductivity type occurs. The measurement of the layer resistance, performed with a four-point probe, is a control measurement after each diffusion process, which provides information not only on the value of R_ρ but also on the homogeneity of the impurity distribution on the whole surface of the Si plate. Most of the producers currently perform doping of the n-type area with the value of R_ρ at the level of 40 ÷ 50 Ω/□, where the fast development of paste production technologies and metallization processes of front electrode contacts makes it possible to produce a cell with the thick film technology for R_ρ ~ 80 Ω/□. In the diffusion process, the doping takes place on all sides of the plate. The elimination of the short-circuit on the edges in the thick film technology is performed in the process of chemical etching of the edges, cutting the latter off with the use of laser or plasma etching.

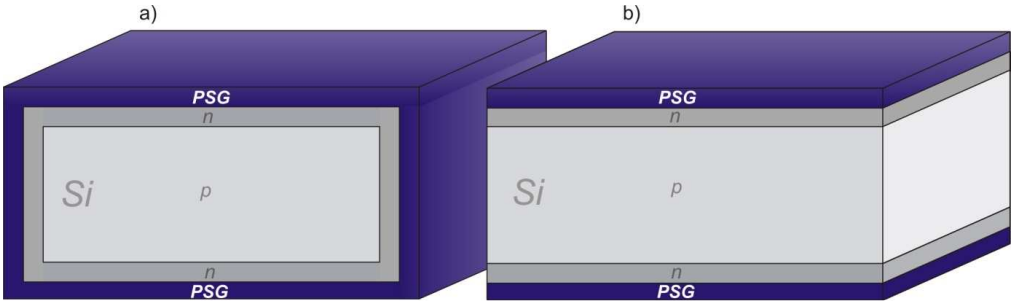

Fig. 16. Cross-section of a plate after diffusion (a) and after edge separation (b).

III. Deposition of passivation and antireflection coating

After separating the edge and eliminating the PSG glass layer in a 5% HF solution, a passivation and an antireflection coating (ARC) is deposited on the front surface of the plate. As the passivation coating, we can apply a SiO_2 layer, produced in dry oxygen at the temperature of 800 ^oC, and next, as the ARC coating, one can deposit e.g. a titanium oxide TiO_2 layer. The mass production of solar cells currently involves the application of only one layer which plays both functions, i.e. a coating of hydrogenated silicon nitride deposited with the method of RPECVD (Remote PECVD) in which the plasma generator is localized beyond the reaction chamber and which allows for the coating deposition at the rate of 2 nm/s. The optimal Si_xN_y:H layer is of the thickness d ~ 85 nm and its refractive index has the value of n ~ 2,05. The above layer also has 10 ÷ 15 % at. H, and this hydrogen, in the process of contact metallization, passivizes the broken surface bondings, and in the case of m-Si – also the grain boundary areas.

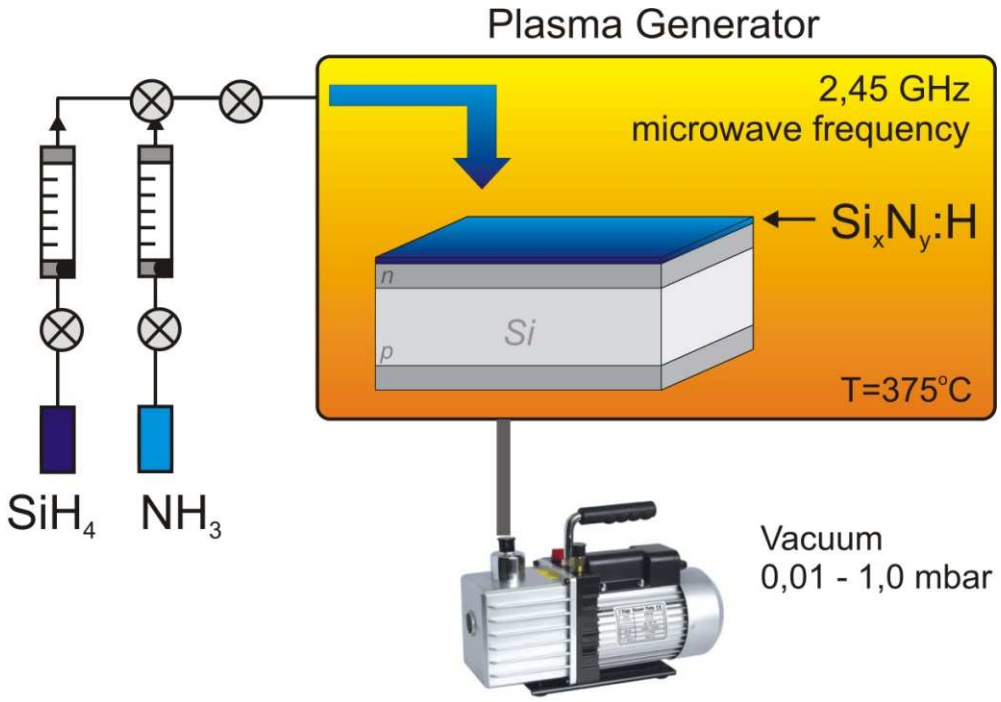

Fig. 17. Scheme of the RPECVD method of deposition a Si_xN_y:H layer formed as a result of decomposition of silane SiH_4 and ammonia NH_4, in which only the ammonia is decomposed into plasma, in the generator located outside the reaction chamber.

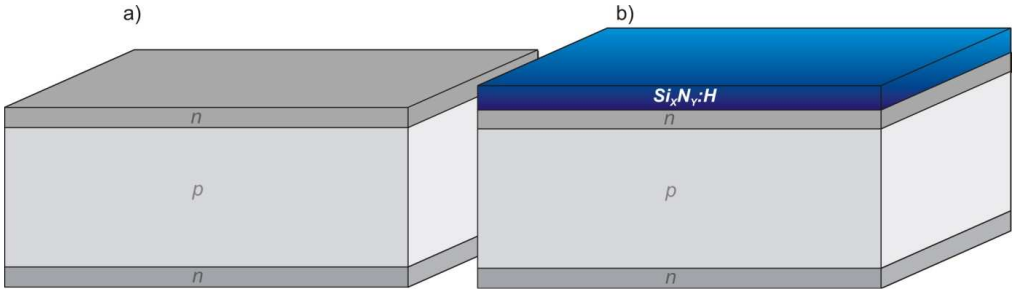

Fig. 18. Scheme of a plate section after the elimination of phosphosilicate glass (a) and after the deposition of a hydrogenated silicon nitride Si_xN_y:H (b).

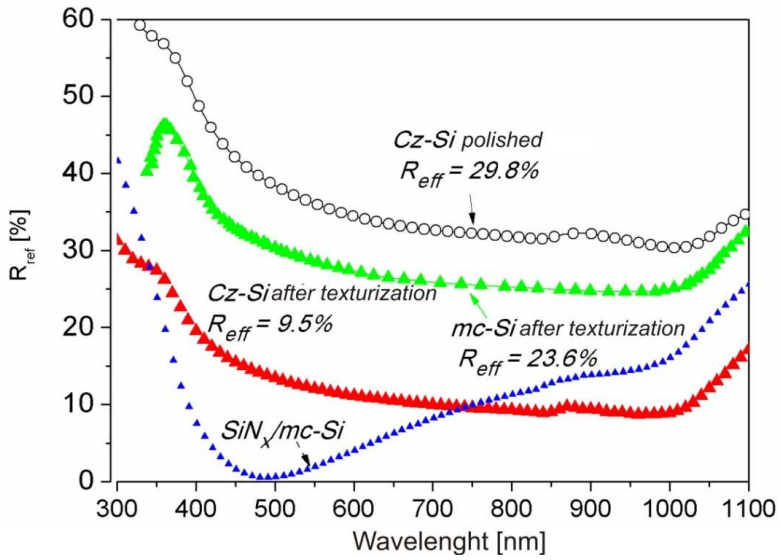

Fig. 19. Dependence of the reflection coefficient on the wavelength for surface-polished silicon Cz-Si and mc-Si, after texturization and deposition of a silicon nitride ARC layer; measurements performed with a spectrophotometer Perkin-Elmer Lambda-19, at AGH, Krakow.

IV. Screen printing process deposition of front and back electrode of the cell

In order to create electrical contacts of the cell, its front and rear surface is coated with pastes with the screen process method, whose automation makes it possible to print 1500 plates per hour, at a single station. The biggest producer of pastes applied in photovoltaics is currently Du Pont. The determined scheme of the deposited paste is the image of a pattern existing on a steel sieve, usually of the density of 280 ÷ 320 msh, where the number of msh denotes the number of the sieve meshes for a distance of 1 inch. The width of the front collecting electrode usually equals 2 mm, and in the case of thin collecting electrodes, this value is from 80 to 120 µm, with a parallel spacing every 2,7 mm. The width and the spacing of the paths is a compromise between the minimization of the component R_4 of the cell's series resistance and the surface area of the cell's front side's coverage with electrodes, the, so called, cover coefficient. In the case of standard cells (Figure 10), the value of the cover coefficient is within the range of 5 %. After the deposition of paste on the given side of the plate, the latter is dried at the temperature of 150 ^{o}C, for 15 minutes, and this process is repeated on the opposite side. The rear surface of the cell is additionally covered with an Ag + 2 % Al strip, which allows for a solder seal, which is not possible in the case of the Al layer covering the remaining part of the surface.

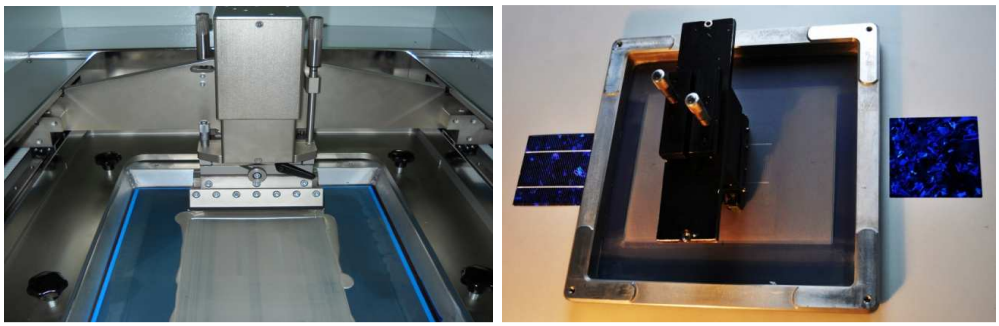

Fig. 20. System of squeegees brushing the paste over the sieve and pressing the paste through the meshes onto the plate's surface (left) and a sequence of paste printing in the process of creating the front electrode with the screen process method (right).

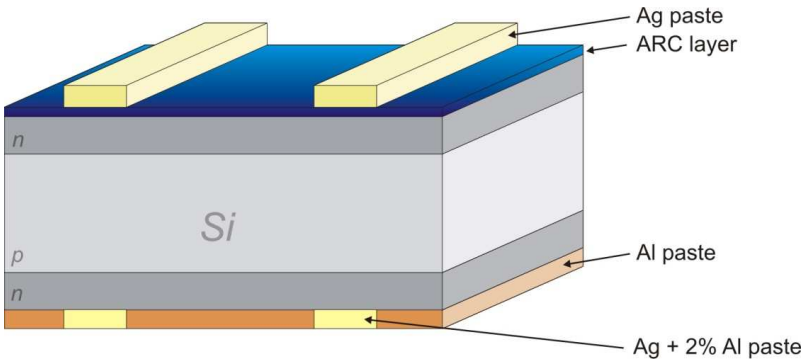

Fig. 21. Scheme of a plate section after the deposition of consecutive paste layers with the screen process method.

V. Thermal process of electrode metallization

After drying the paste, the plate is fired in an IR furnace, in purified natural atmosphere or in N_2. The actual temperature of the electrode metallization process depends on the temperature in the particular consecutive heat zones of the furnace and the speed of the tape transport. The temperature profile of the metallization process must be set in such a way so that the Ag paste can penetrate the Si_xN_y:H layer and create an alloy with the upper Si emitter layer of the n-type, but which can absolutely not diffuse inside the area of the space charge. At the same time, in this process, at the temperature of above 577 ^{o}C, Al diffuses from the paste deposited on the rear surface of the plate, at the depth of about 5 µm, and compensates the existing area of the n-type conductivity and the thickness of ~ 0,5 µm, changing the conductivity type into p, with a simultaneous formation of the Al-Si alloy. A part of the diffusing Al atoms assumes the substituting positions in the crystal Si lattice,

which results in the formation of a local layer with the conductivity of the p^+ type, often called the BSF layer (Back Surface Field).

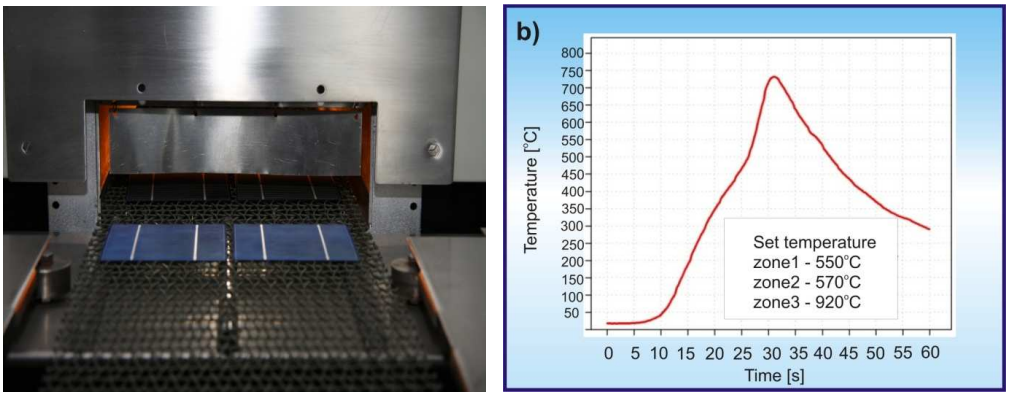

Fig. 22. A silicon plate placed on the tape entering the IR furnace and the temperature distribution profile of the plate during its crossing at the rate of 200 cm/min through a 2 m long furnace with heat zones at the distance of 36 cm (b).

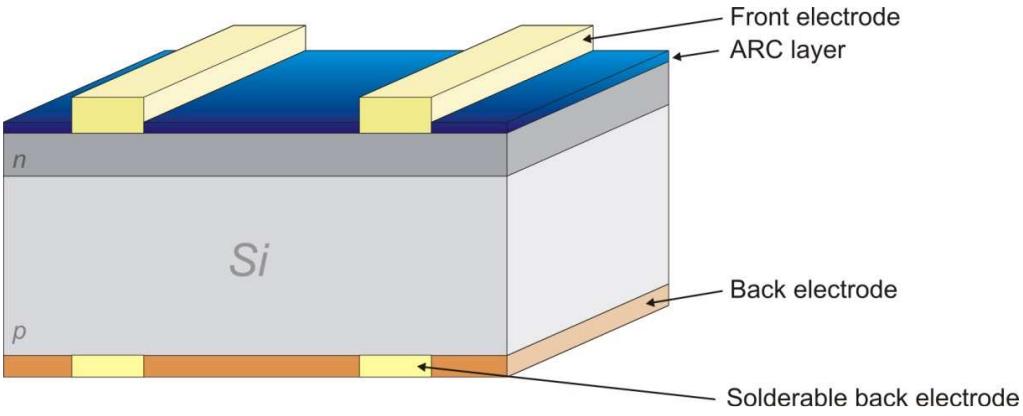

Fig. 23. Scheme of solar cell section after metallization.

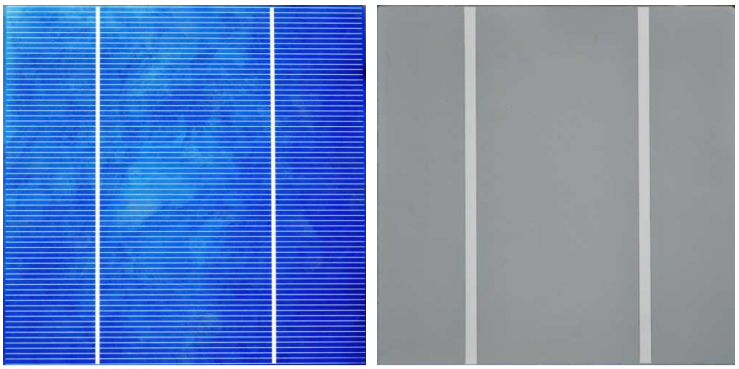

Fig. 24. Front (a) and rear side of the solar cell (b) with the surface area of 164 cm^2, produced on mc-Si silicon, with the construction adequate to the scheme in Fig.23.

VI. Current-voltage characteristics measurements

One of the basic measurements of photovoltaic cells is the measurement of the light current-voltage characteristics (I-V). In the measuring system, one can distinguish three basic elements which determine the measurement quality, that is the light source, the measuring system, as well as the table and the contact probes. The I-V characteristics must be measured under strictly defined conditions for the given radiation spectrum and temperature, under so called STC (Standard Test Condition). The applied standard also includes the use of solar light simulators Class A, with the AM1.5 spectral matching tolerance within the rage of 0,75 ÷ 1,25 and with the acceptable inhomogeneity of the illumination intensity of ± 2 %, on the surface of the solar cell illuminated by the radiation with the intensity of 1000 W/m^2, and with the temperature of the cell equaling 25 ^oC [58].

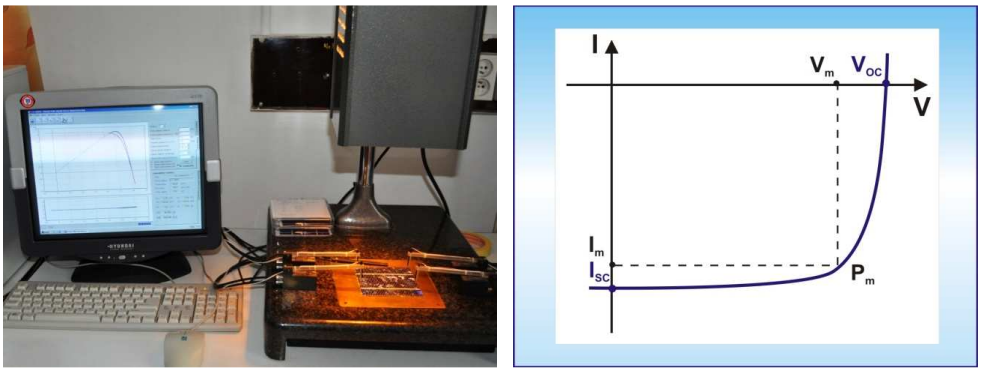

Fig. 25. Solar simulator and I-V characteristic of a illuminated solar cell.

The numerical matching of the I-V characteristics with a single or double diode model makes it possible to calculate directly the value of the photocurrent, the voltage, the dark current, as well as the parallel and series resistance of the cell [59].

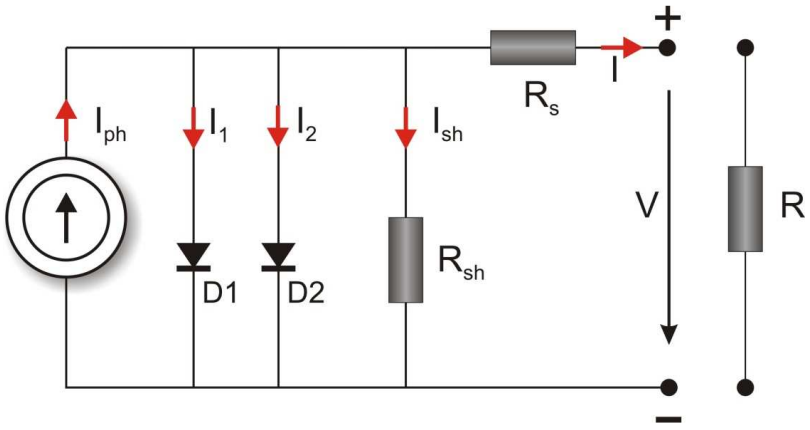

Fig. 26. Scheme of the equivalent electrical circuit in a double diode model for an actual silicon solar cell; designation in accordance with the dependence (20).

The mathematical model which most thoroughly describes the non-linear I-V characteristics of a solar cell is the equation (20) with seven parameters, which one can obtain by applying Kirchhoff's Law to the equivalent circuit presented in Fig. 26 [60].

$$I = I_{ph} - I_{S1}\left[\exp\left(\frac{q(V+IR_s)}{A_1kT}\right)-1\right] - I_{S2}\left[\exp\left(\frac{q(V+IR_s)}{A_2kT}\right)-1\right] - \left(\frac{V+IR_s}{R_{sh}}\right) \qquad (20)$$

or

$$I = I_{ph} - I_1 - I_2 - \left(\frac{V+IR_s}{R_{sh}}\right) \qquad (21)$$

and

$$I_1 = I_{S1}\left[\exp\left(\frac{q(V+IR_s)}{A_1kT}\right)-1\right] \quad , \quad I_2 = I_{S2}\left[\exp\left(\frac{q(V+IR_s)}{A_2kT}\right)-1\right] \qquad (22a)\text{ , }(22b)$$

where:

- I - current possible to obtain from the solar cell
- I_{ph} - photocurrent generated by electromagnetic radiation
- I_1 - dark diffusion current
- I_2 - dark generation-recombination current
- I_{S1} - saturation current of dark current diffusion component
- I_{S2} - saturation current of dark current generation-recombination component
- V - voltage possible to obtain from the solar cell
- R_s - cell's series resistance

I_{sh} - leakage current
R_{sh} - cell's parallel resistance
A_1 - diode's quality coefficient (value close to 1)
A_2 - diode's quality coefficient (value close to 2)
R - external resistance

Parameter I_{sc} is described as the short-circuit current, and V_{oc} is the voltage of the open circuit. The I-V characteristics presented in Fig. 25 include the points which determinant for the cell's photovoltaic conversion efficiency E_{ff}. The value of $P_m = I_m \cdot V_m$ is the maximum actual power possible to be obtained from the cell, but always lower than the ideal maximum power being a product of $I_{sc} \cdot V_{oc}$, which is expressed by the filling factor FF in the relation [17]:

$$FF = \frac{I_m V_m}{I_{sc} V_{oc}} = \frac{P_m}{I_{sc} V_{oc}} \tag{23}$$

Knowing the above I-V characteristics, one can calculate the basic and most important value for the solar cell, which is the value of its photovoltaic conversion efficiency E_{ff}, often described as the cell efficiency, according to the following formula [17]:

$$E_{ff} = FF \frac{I_{sc} V_{oc}}{P_{in} A_0} \cdot 100\% \tag{24}$$

where: P_{in} - intensity of radiation falling on the cell [W/m^2]
A_0 - cell's surface area [m^2]

This is one of the most important quantities determining the market price of the cells sold as commercial product, whose value is given in Euro (€) or USD ($) per watt of the cell power. The decisive factors for the shape of the I-V characteristics are the quantities R_s and R_{sh}, which is presented in Fig. 27, with the following marked values: $P_m(R_s)$ – maximum cell power with excessive R_s, $P_m(R_{sh})$ – maximum cell power with deficient R_{sh}.

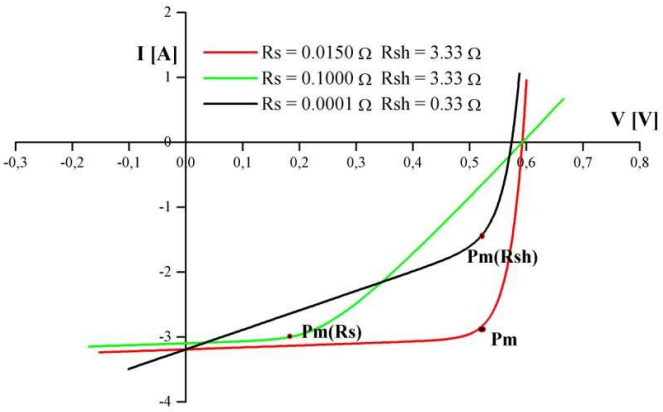

Fig. 27. Effect of the series R_s and parallel R_{sh} resistance on the light characteristics of a solar cell. Dependences calculated with the PC-1D computer software, with the established values of R_s and R_{sh} for a 100 cm^2 cell.

In both cases, $P_m(R_s)$ and $P_m(R_{sh})$ are much lower than P_m, due to the effect of the cell's series and parallel resistance on the latter's filling factor and the related efficiency, according to the formula (24). The power quoted by the producers of cells and modules refers to the point P_m, determined with the STC measurement, and to distinguish this fact, photovoltaics applies the quantity W_p (Watt peak), instead of W.

The basic fundamental factor conditioning the value of the power P_m, possible to obtain from the cell, under the latter's external work, is the spectral power and characteristics of the solar radiation falling on the cell. Figure 28 presents the energy spectrum of solar radiation, under the conditions AM1.5.

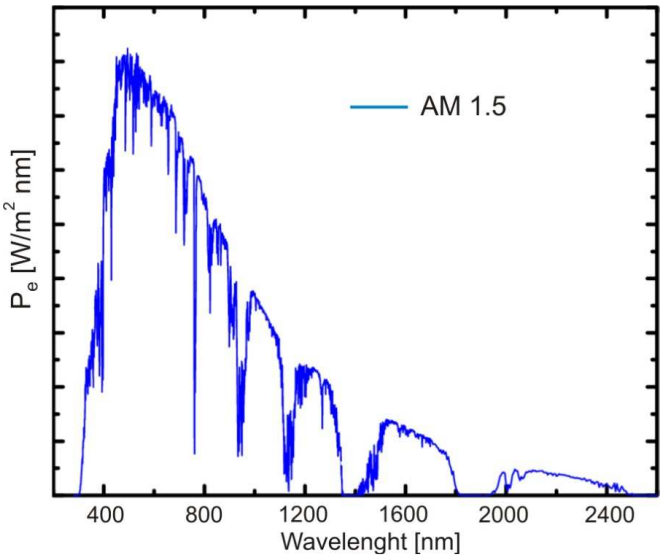

Fig. 28. Spectral distribution of solar radiation under conditions AM1.5, where P_e is the density of the solar radiation's monochromatic flux.

The number of the air mass AMm is the function of the angle α, formed between the direction of the Sun and the direction of the zenith, according to the dependence $m = (\cos\alpha)^{-1}$. For the solar radiation beyond the earth's atmosphere, the conditions are described as AM0, and for the radiation at the sea level, where the Sun is in its zenith, the conditions are AM1. In the case of crystalline silicon, the radiation with the wavelength above 1,1 µm will not generate charge carriers, and thus it will be lost for the solar cell. The spectrum availability for a given type of semi-conductor material with the energy gap E_g, that is the long-wave border, below which it is possible for an electron to transfer from the valence band to the conduction band, can be calculated from the following dependence:

$$\lambda = hc/E_g \qquad (25)$$

where: h – Planck's constant
c – light velocity

The application of the above dependence allows for a significant increase of the solar cell's photoconversion efficiency with the use of materials of different energy gap values E_g. This principle is the basis for multijunction cells, usually produced on the GaAs base, in which consecutive layers, placed from the rear to the front side of the cell, possess progressively larger value of E_g.

The measurements of the I-V characteristics are the more precise and unique, the more the radiation spectrum of the solar simulator lamp resembles the actual

spectrum of solar radiation for the given AMm conditions, which is achieved with the use of xenon arc lamps in the best Class A simulators.

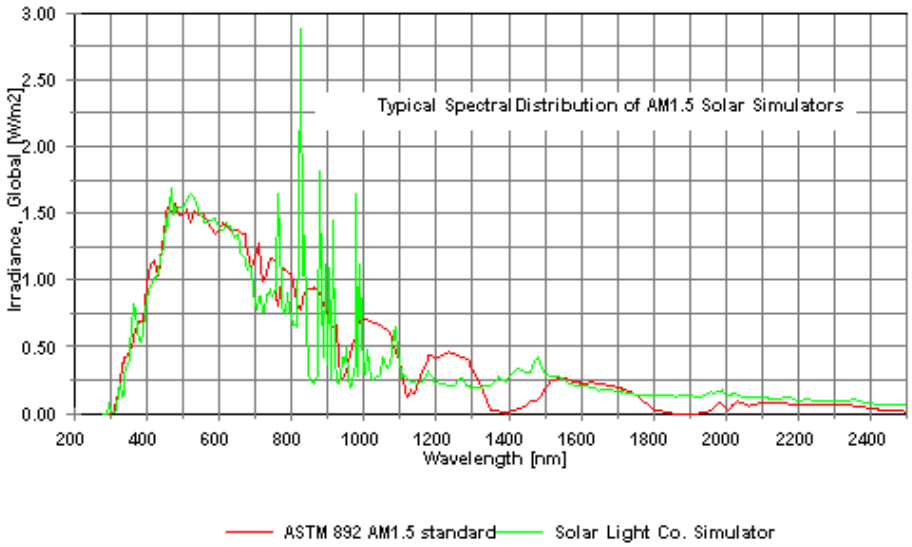

Fig. 29. Comparison of the solar radiation distribution under conditions AM1.5 with the radiation distribution of an arc xenon lamp used in the solar simulator LS1000 produced by Solar Light Company Inc., Glenside, USA [61].

2.6 Directions of silicon solar cell development

The basic trend in the research and development work is the reduction of the thickness of the solar cell's base plate, from the currently applied 200 ÷ 150 µm down to 80 ÷ 120 µm, with a simultaneous reduction of the material lost in the process of cutting a single plate from a block, from the present 150 ÷ 120 µm down to 80 µm. This requires a full automatization of the production processes. Theoretically, the calculated efficiency of the photovoltaic conversion for silicon solar cells can reach the value of 32,9 %, with the assumption of a full absorption of radiation and the presence of only the radiant combination [62], whereas in the case of the assumed Auger recombination, the efficiency can achieve the value of 29,8 % [63]. This leaves a significant space for the concepts of solar cells allowing for a greater conversion efficiency E_{ff} than that of the cells currently manufactured in the mass production, with the efficiency of 16 ÷ 19 %, type PESC *(Passivated Emitter Solar Cell*), whose scheme is presented in Fig. 10. One of the leading silicon solar cell development centers is the University of New South Wales, Australia, where, in 1999, the team under the direction of Martin Green obtained an FZ-Si solar cell of the world's highest conversion efficiency, that is 24,7 % [64]. It is a PERL-type cell *(Passivated Emitter*

Rear Locally diffused). Although it is made on a 4 cm^2 plate, its basic parameters, such as: V_{oc} = 0,706 V, J_{sc} = 42,2 mA/cm^2 i FF = 0,828, determine the level of values to which one should refer their results in the field of silicon cell construction. The cell, manufactured in the photolithographic technology, has such excellent parameters due to the following factors: a very small value of the reflection coefficient ~ 2 %, obtained as a result of selective etching of the front surface, a high resistance of the n-layer between the front contacts – above 200 Ω/□, an additional donor impurity of the n^+-type under the front contacts and an additional acceptor impurity of the p^+-type under the local rear contacts. One of the more interesting concepts are the cells with buried contacts, type BCSC *(Buried Contact Solar Cell),* which have been produced since the beginning of the 1990s, under license of the English company BP Solar [65].

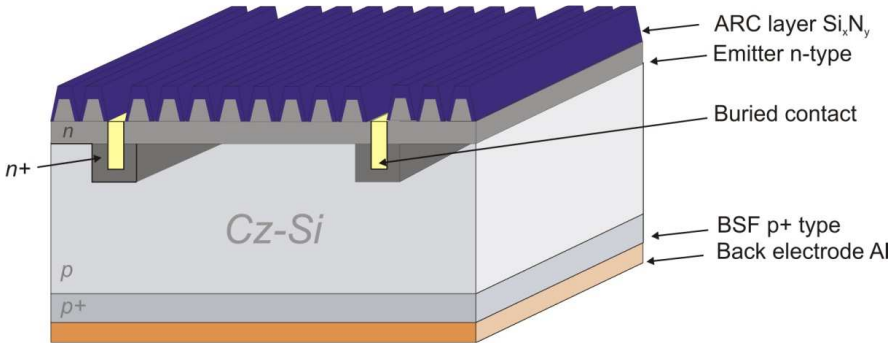

Fig. 30. Cross-section of a mono-crystalline silicon solar cell with buried contacts (BCSC).

The highest conversion efficiency, 22 %, was obtained for a mono-crystalline BCSC cell, type FZ. The basis for achieving such a high efficiency is the application of the front electrode contacts made of a nickel-copper-silver layer, deposited by means of a chemical bath in the ~ 30 ÷ 50 µm deep laser-cut grooves. Applying a second donor diffusion through the mask makes it possible to create a strongly doped n^+-type area under the contacts, with the laminar resistance at the level of 20 Ω/□, which affects the reduction of the series resistance. The high-resistant emitter R_ρ ~ 120 ÷ 200 Ω/□, between the thin leading electrodes, reduces the disadvantageous effect of the Auger recombination process and allows for a significant improvement of the cell's current density.

Another cell type, combining the mono-crystalline silicon with the amorphous one, is the HIT-type solar cell *(Heterojunction with Intrinsic Thin layer)*, whose construction scheme is presented in Fig. 31.

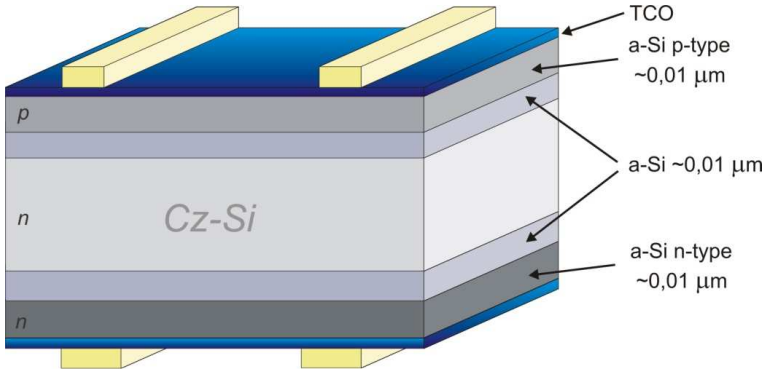

Fig. 31. Cross-section of a mono-crystalline solar cell with double-sided layers of amorphous silicon (HIT) [66].

The efficiency of the HIT-type cells is the result of the excellent passivation of the silicon's surface, provided by the non-doped layer of hydrogenated amorphous silicon, which reduces SRV down to the level of 30 – 50 cm/s (Table 9). What is more, the whole of the technological processes of the solar cell production is performed at the temperature below 200 ^{o}C, which does not cause the generation of additional recombination centers or silicon defects [67].

The direction of research aiming at the achievement of the highest possible photovoltaic conversion coefficient with the minimum thickness of the crystalline plate, generates a significant problem resulting from the fact that the 30 µm-thin aluminium layer, used to obtain the rear contact, deposited with the screen printing method, causes the thin Si plates to bend and break, due to the difference in the thermal expansion coefficient, which equals 2,35x10^{-6} K^{-1} for Si and 25,3x10^{-6} K^{-1} for Al. What is more, the generated back Al layer has its reflection coefficient, within the longwave range, only at the level of 70 – 80 % and it allows for the SRV reduction on the back surface only down to the value of about 500 cm/s. Considering the above facts, one of the solutions is the passivation of the back surface of the cell and the creation of point contacts with the use of laser, which will allow to maintain a large fraction of the rear surface with the passivizing layer. This is implemented in the case of the LFC cells [68]. A single contact point is a few hundred micrometers in diameter, and the distance between the consecutive points is within 1 mm.

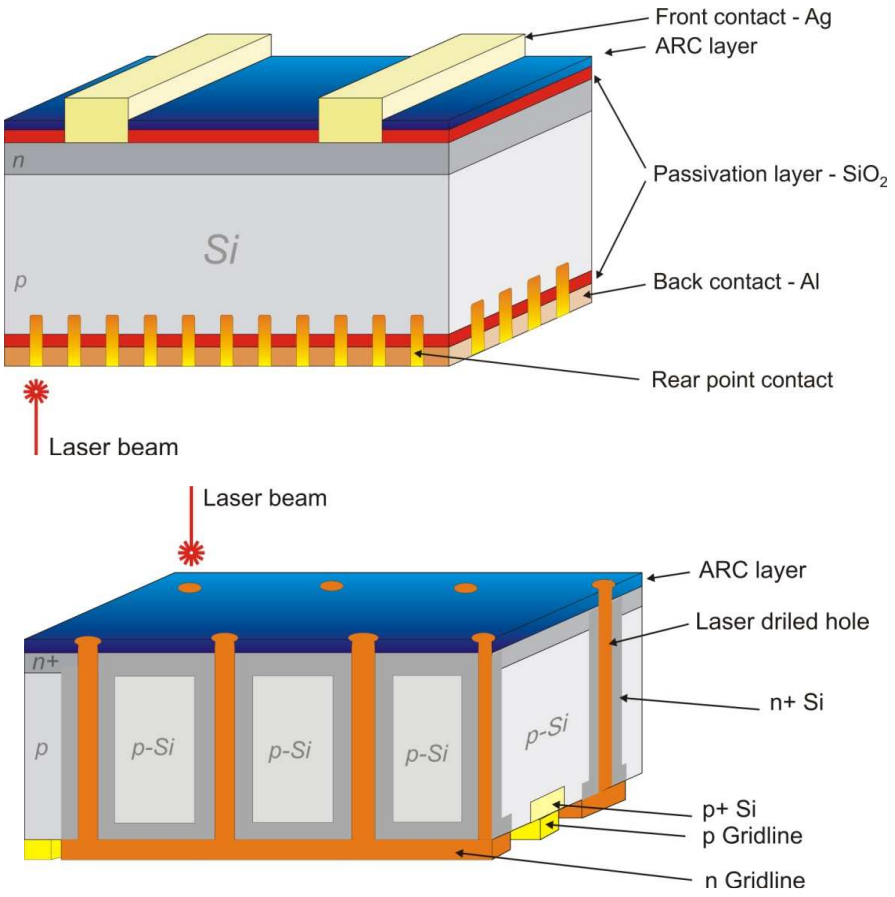

Fig. 32. Cross-section of a solar cell with rear point contacts, produced with the laser LFC *(Laser Fired Contact)* method, and cells with an EWT *(Emitter Wrap Through)* emitter.

The EWT-type cells are produced by Photowatt [69]. Their most important distinguishing mark is the few hundred holes, ~ 100 µm in diameter, produced with the use of laser, whose wall-doping is the same donor type as that of the emitter, and this allows to localize the electrode contacts exclusively on the back side of the cell. This reduces the cover coefficient down to zero, which, in turn directly affects the increase of the short-circuit current's density J_{sc} of the cell. An additional advantage of the cells with the contacts localized only at their back side is the possibility of their assembly into a module without the sequential interweaving of the connection strips, which allows for a better packing of the cells and also creates the possibility of an integrated module assembly, that is soldering the cell layer with the previously prepared rear matrix of the module.

Next to the few exemplary types of solar cells discussed above, there is a wide range of other kinds of photovoltaic converter constructions, such as the MIS cells *(Metal Insulator Semiconductor)* or the SIS cells *(Semiconductor-TCO Insulator Semiconductor)* [17].

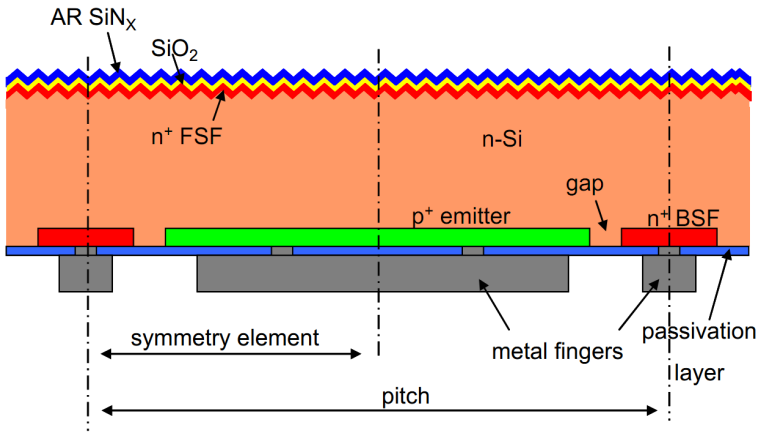

Fig. 32a. Schematic cross-section of the n-type high-efficiency back-contact back-junction silicon solar cell. [85]

Another type of high-efficiency solar cell is n-type back-contact back junction solar cell. A schematic cross-section of this type of cell is shown in Figure 32a. The cells is fabricated using n-type, FZ silicon wafers. The thickness of the finished solar cells is about 160 µm. The front side is textured with random pyramids and passivated. The front is lightly doped by phosphorus N_{peak} = 5×10^{18} atom/cm^3 but deeply diffused x_c = 1.4 µm, what effects that sheet resistance is around 148 Ω/sq. The diffusion profile must be optimized to achieve an optimum front side passivation quality. Specific base resistivities of this type of cell are in the range from 1 to 8 Ω cm. This, specific base resistance, range is believed to be an optimum between two effects: maximization of the carrier lifetime in bulk and reduction of the series resistance losses introduced by the base material (see equation 13). On one hand, the carrier lifetime, which needs to be high in order to enable good collection of the minority carriers at the rear junction, decreases with increased base doping level and reduced specific base resistance of the base material. On the other hand, the high specific base resistivity results in increased series resistance in the base material, which leads to significant efficiency losses. [85]

In the industry, the highest commercially available solar cells are produced on n-type Si substrates. SunPower Corp. produces back-contact back-junction n-type Si solar cells with efficiencies up to 22.7 % [86].

3. Thin-layer cells and modules

Among the thin-layer solar cells, those of the greatest importance are currently the cells with a cadmium telluride base (CdTe), the latter having a simple energy gap E_g = 1,48 eV and a high value of the absorption coefficient $\alpha \sim 10^5$ cm^{-1}, within the wavelength range of 300 ÷ 820 nm, which makes the layer, only a few micrometers thick, provide the absorption of almost all the radiation in the above range [70]. The structure of the CdTe-type cell is shown in the scheme in Fig. 33. The above cells are made with the method of depositing successive layers on a glass base covered with a thin layer of a transparent conductive oxide (TCO). The rear contact is achieved through a thin layer of metal. The significant advantage of such cells is the possibility to produce their successive construction layers by means of such techniques as a chemical bath, vapour deposition, electrolysis, magnetron sputtering, spraying or close space sublimation (CSS) [2]. The structure deposited on the surface of the glass, which, at the same time, determines the size of the thin-layer module, is separated through laser cutting into single cells, which, connected in series, provide the proper value of the module's voltage.

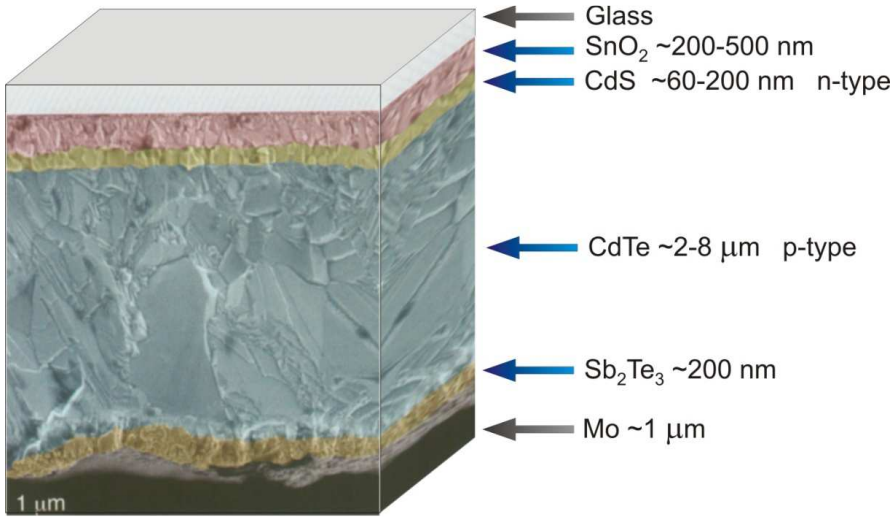

Fig. 33. Cross-section of a thin-layer CdTe cell with a typical kind of conductivity and thickness of particular layers [71].

The possibility of a continuous line of ready-made PV module manufacturing, at the temperature not higher than 625 °C, with the CCS method used for the polycrystalline CdTe layer deposition, makes the production price 1 $ per 1 W_p

of power. The world-wide leader in producing CdTe modules is First Solar (USA). Some market uncertainty is, however, risen by the possibility of a ban introduction on the cadmium usage in the EU, planned for 2026. A significant factor is also the necessity of a one-time investment of the order of 120 – 150 mln $ in the power line of 50 MW_p per year, whereas the same volume of the produced power in the case of crystalline silicon-based cells requires an investment of the order of 35 mln $ - in the production of silicon and plates, 25 mln $ - in the production of cells, and 10 mln $ - in the final module assembly.

The polycrystalline component semi-conductor, which is $CuInS_2$ (CIS) or $Cu(In,Ga)Se_2$ (CIGS), is next to CdTe, the most important material applied in photovoltaics for thin-layer cell production [70]. Its high absorption coefficient makes the CIGS layer, only 0,5 µm thick, absorb about 90 % of the solar radiation. Similarly to the CdTe modules, the integrated CIGS modules are manufactured in continuous processes, with the application of the same methods of successive layer production [72]. Not particularly advantageous in the case of the CIGS-type cells is the drop of the initial efficiency of the photovoltaic conversion, which, after ten years, becomes reduced down to 90 % and after twenty-five years – down to 80 % of the original efficiency, although, in comparison to other thin-layer cells, the degradation level is lower. The biggest producer of the above cells is Wurth Solar (Germany).

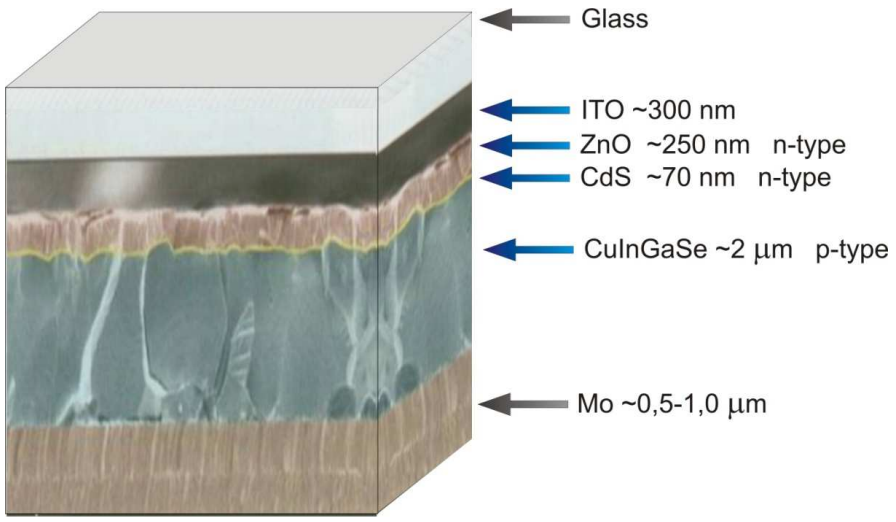

Fig. 34. Cross-section of a thin-layer CIGS cell with a typical kind of conductivity and thickness of particular layers.

The amorphous (a-Si) silicon-based cells are mainly applied in devices of low power consumption, such as calculators and watches. Despite the fact that it has

been almost 30 years since the first solar cells were obtained, so far, there has been no success in solving the basic problems causing the a-Si module efficiency to remain at a relatively low level, of about 5 %, and also, after a few months of outdoor operation, their photovoltaic conversion efficiency to drop down by about 15%. The a-Si cells are produced with the PECVD method and, similarly to other thin-layer cells, are obtained in the form of integrated modules. Due to the disordered crystalline structure of amorphous silicon, E_g is not strictly determined, although generally, it assumes the values of 1,7 ÷ 1,8 eV [70]. For the absorption of the available spectral range, a non-doped (i) a-Si:H-type layer, about 300nm thick, is introduced between the thin doped ones. The illumination of the (i) a-Si:H layer causes, however, its degeneration, as a result of the bonds breaking between the hydrogen and the silicon, which effects a drop of the photovoltaic conversion efficiency of the cell. One of the concepts are hybrid a-Si/µc-Si cells manufactured by Kaneka, Japan, which is planning its production development at the level of 130 MW per year [6].

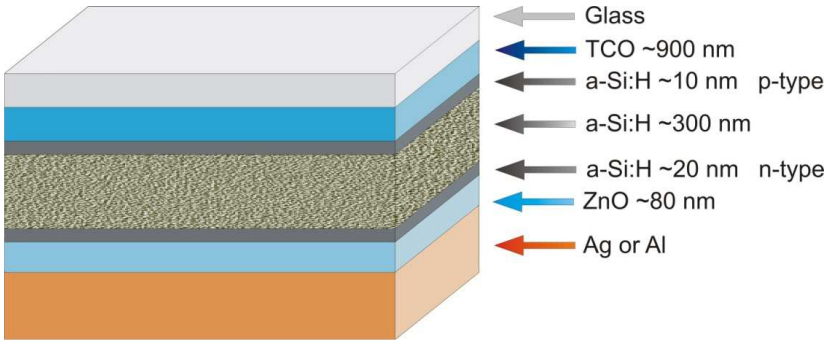

Fig. 35. Cross-section of a thin-layer cell made of amorphous silicon, with a typical kind of conductivity and thickness of particular layers.

The basic drawback of all types of thin-layer cells, that is the cells whose active layers are a few micrometers thick, are the difficulties in determining the standard power and energy output, resulting from the metastable processes taking place in their absorbers and causing a fluctuation of the initial parameters, under the effect of many factors, such as the illumination time or the dark room storage time.

4. Photovoltaic modules

A solar cell, as a single converter of solar radiation energy into electric energy, has a specific voltage value at the external terminals, and it can be the source of current I_{sc} with the intensity directly proportional to the illumination intensity P_{in}. The voltage at the opposite poles of a single solar cell will have the same value, independently of the active surface of the cell, and the value of the current intensity possible to obtain from a single cell will be directly proportional to its surface area. As it results from the dependence presented in Fig. 36, contrary to the case of the current intensity, the value of the cell's voltage, depending on the illumination intensity, changes in a non-linear manner and only for a very small value of P_{in} it drops down to zero. This, for the typical daily values of the illumination intensity in Poland, which vary from 200 W/m^2 to 1100 W/m^2 in winter and summer months, respectively, prevents the cell's voltage value from significant fluctuating. The above dependence will, of course, also apply to the series and parallel-connected cells.

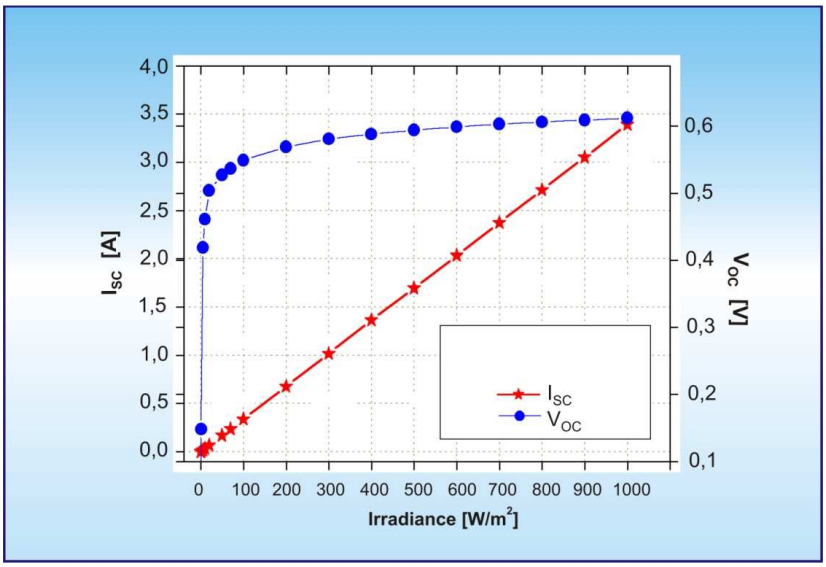

Fig. 36. Dependence of a solar cell's open circuit voltage (V_{oc}) and its short-circuit current (I_{sc}) on the illumination intensity. Calculations performed with the PC-1D computer software for a 100 cm^2 Cz-Si cell.

The combination of a series or parallel connection of single solar cells makes it possible to obtain a generator of the required value of intensity and voltage, which is schematically shown in Fig. 37. A typical Cz-Si-based p-type cell with an n-type emitter, due to the fact that it works in the backward direction, it has a negative

electrode on the front side and a positive one on the back side. The cells are connected with thin copper strips, 2 mm wide and 0.15 mm thick, coated with the Sn62%Pb36%Ag2% tin alloy.

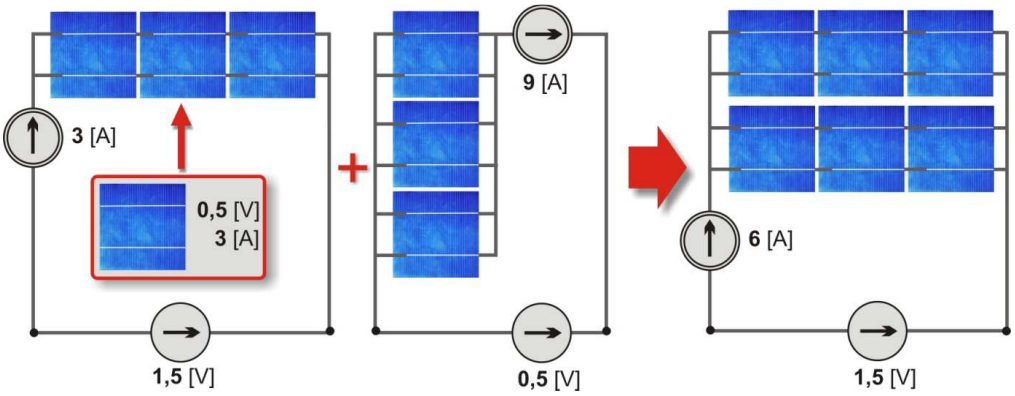

Fig. 37. Techniques of connecting solar cells; the initial values of the current intensity at the point of maximum power (I_m) and of the voltage at the point of maximum power (V_m) for a series and parallel sequence of several single mc-Si cells with the surface area of 100 cm^2.

As single solar cells are electron devices of a very fragile construction, the cells connected in series or in parallel are hermetized in the process of lamination into photovoltaic modules. Only the module is an element which can be applied as a practical and useful source of direct current, under all kinds of atmospheric and terrain conditions. Most of the industrial mc-Si and Cz-Si modules are manufactured out of 36 or 72 solar cells connected in series, in such a way so that the module's voltage V_m is higher than the rated voltage required to charge a typical 12 or 24 volt accumulator. The cells for the given module are selected according to the value of I_m, yet one should also take into account the value of R_{sh} [73]. The construction of a typical PV module is a sequence of component layers, which is presented in Fig. 38.

Fig. 38. Construction layers of a crystalline silicon-based photovoltaic module.

In order to provide a long-term protection for a PV module under the conditions of outdoor operation, the producers apply protective layers as panels made of tempered glass, 3 mm thick, with the transmission coefficient T of above 94 %. The foils used as laminates are made of transparent materials type PVB (polyvinyl butyral) or EVA (ethylene vinyl octane). The rear protective foil is usually a white or coloured teflon foil type PVF (polivinyl fluoride). The lamination process takes place in a chamber, from which the air is pumped off, and additionally, the layer system of the module is pressed down with a teflon membrane and heated up to about 150 ^{o}C for a minimum period of 12 minutes. A properly performed lamination process must provide polymerization of the EVA foil of above 70 %.

Fig. 39. Laminator L200, by the Italian producer Penergy, with an open lid of the heating chamber and a prepared system of layers for the lamination of a PV module, 50 cm wide and 100 cm long.

The biggest global producer of components applied in photovoltaics in the lamination process of PV modules is Du Ponte.

5. Photovoltaic systems

Photovoltaic systems are electric systems which make it possible to practically utilize the energy of solar radiation. The power of these systems can be within the range from a few W_p to a few hundred MW_p, which determines their structure and configuration. The simplest autonomous photovoltaic system consists of a photovoltaic module, a voltage controller and an energy receiver. Due to their little usefulness, resulting, among others, from their effective work only when illuminated, the practically applied autonomous PV systems consist of PV modules, a charging controller, an accumulator and an energy receiver. The charging controller is used in small autonomous systems with the power up to a few kW_p and its purpose is to supervise the charging process of the accumulator, in order to switch off the charge above 13,7 V and to switch off the accumulator's loading below 11,1 V. The current obtained from the PV module is a direct current (DC) and thus, in the case of the use of an electric energy receiver, which requires an alternating current (AC) supply, it is necessary to apply an inverter in the PV system.

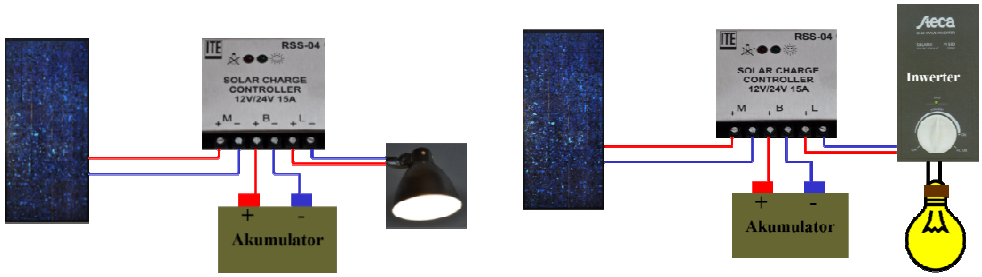

Fig. 40. Scheme of an autonomous PV system type DC (a) and type AC (b).

The most important categorization of photovoltaic systems classifies them as the autonomous systems and the integrated systems with an energy network. In the case of the autonomous systems, their power can vary from a few W_p to a few kW_p, and as for the integration with the energy network, this case is appropriate for the systems with the power above 3 kW_p. Within the frames of this division, we can distinguish the systems constantly oriented and the follow-up systems, in which the module plane is set mechanically, parallelly to the direct radiation. In the case of the systems integrated with the network, they can be scattered or central, that is, they are big PV electric power stations, the largest of which, with the power of 97 MW, is currently located in the town of Sarnia, Canada. [74]. Typical PV power plants possess the power within the range of 1 ÷ 80 MW_p. Another categorization distinguishes the PV systems as the free-standing ones and those integrated with buildings (BIPV),

in which the PV modules play the role of a facade or a roofing [75]. In justified cases, the photovoltaic systems are combined with a wind power plant or a combustion power generator and classified as the hybrid systems.

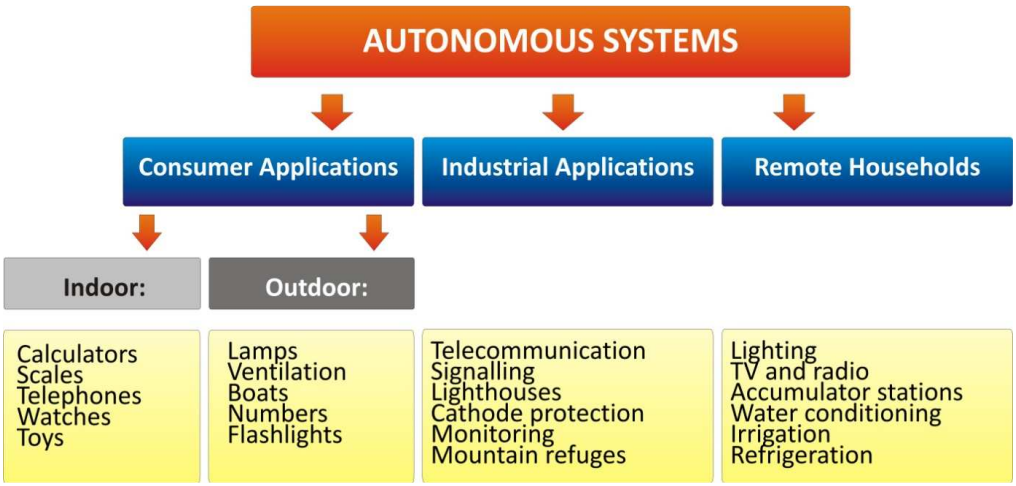

Fig. 41. Classification of the autonomous PV systems and their most popular application areas.

The electrical connections of particular elements of the PV systems are made with the use of polyuretane-isolated conductors, 2,5 mm to 45 mm in diameter, depending on the current configuration of the system. The connection points must be protected from rain and humidity, which is usually realized through additional filling of the hermetic junction boxes with silicon. One of the more important elements of the PV systems type AC is the inverter, which not only changes the current from DC to AC, but it also monitors the operation of the PV system and adjusts the maximum power point of the MPPT *(*Maximum Power Point Tracking*)* system with the use of a controllable DC/DC converter. The efficiencies of inverters are currently at a very high level and they do not cause significant losses during the DC/AC transformations. An exemplary inverter produced by Sunways, designed for the PV systems with the power up to 5 kW, has the efficiency of 97,4 % [76], and the Voltwerk inverters from the WCWL 110-300 series, assigned for the PV systems with the power from 110 to 300 kW, have the efficiency value of 98,8 % [77]. The biggest inverter stations with the power up to 2000 kW have the efficiency of 98,4 % [78]. For the consumers, the most interesting application of a PV system is powering their own apartment building, with the option of selling the electric energy excess to the power network, or, in the case of its lack from the PV system, of using the network energy. Such a system can be equipped with a charge controller and a set of accumulators

providing an autonomous operation at night time. Exemplary schemes of a PV system connected to the power network with a meter system measuring the energy balance are presented in Figures 42 and 43.

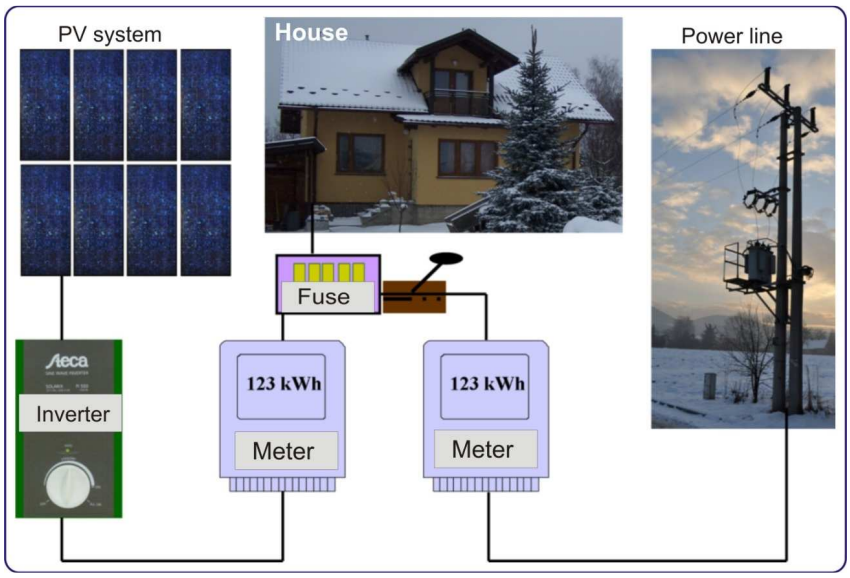

Fig. 42. Scheme of an electric system of a PV system powering a single family house and integrated with one power network phase.

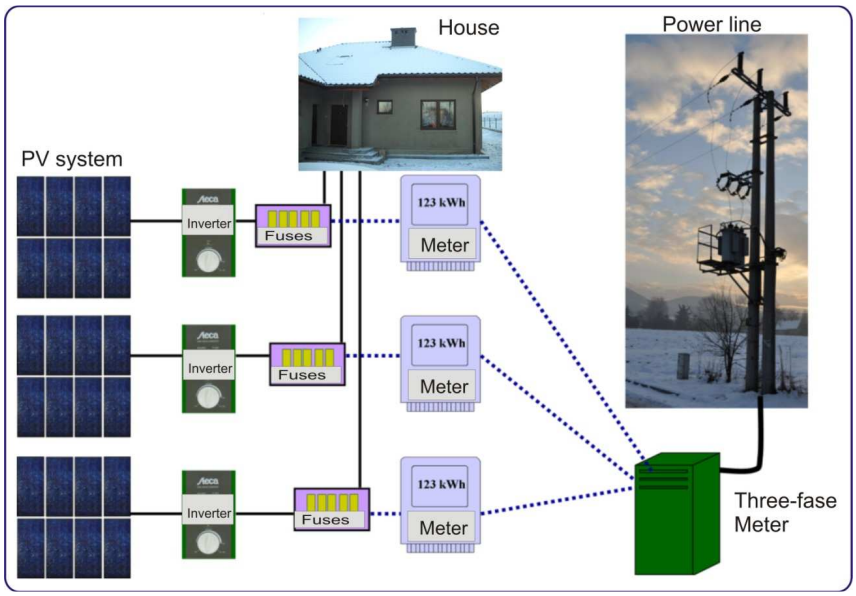

Fig. 43. Scheme of a triphase electric system of a PV system powering a single family house and integrated with the power network.

A set of photovoltaic modules of the PV system powering the triphase current network must be divided into three segments of equal initial power. For the safety matters, the PV system must also have earthing and a lightning arrester installation. The configuration of a chosen PV system and its energy balance can be calculated with the application of the commercially available computer software, such as PVsyst 5.03. [79].

One of the largest PV systems in Poland is located on the roof of a carrying freezer owned by FROSTA in Bydgoszcz. The self-acting system with the power of 80,5 kW_p, constructed on the surface area of 600 m^2, consists of 366 mc-Si modules produced by Conergy and it allows for a 30 % electric energy safe, necessary for chilling the cold store. A big PV system integrated with a 53 kW_p power network, built of a-Si and mc-Si modules, is located on the building of the Faculty of Environmental Engineering, of the Warsaw University of Technology. The largest - 1 MWp - grid connected PV system in Poland is located in Wierzchosławice community

Fig. 44. 80,5 kW_p PV system used by the FROSTA company in Bydgoszcz. (left). Faculty of Environmental Engineering of the Warsaw University of Technology - facade of the building (right). 1 MWp, grid connected PV system located in Wierzchosławice community (bottom)

6. Economical aspects of photovoltaics

The construction of a ready-made market product in the form of a photovoltaic system requires the use of numerous components, of which the solar cell's base material and the cell itself are the most costly and technologically advanced elements. The precisely calculated financial expenditures depend on many economic factors, but some value levels can be estimated on the basis of the available data. The production costs of the crystalline silicon-based photovoltaic module can be divided into: the costs of producing the silicon blocks through casting, the costs of cutting the blocks in plates, the costs of producing the cell and the costs of producing the module. Table 10 includes the above production costs, calculated for the enterprises with the efficiency at the level of 30 ÷ 50 kW_p per year, with the assumed price of the polycrystalline charge material obtained in the Siemens process to be 40 €/kg. The table designates the human labour as „labour" and the „losses" section includes the proportional efficiency of a given process.

Tab. 10. Component costs in €/W_p for particular stages of producing 1 W_p of power of a photovoltaic module with the efficiency of 14,5 % made on the basis of six-inch mc-Si silicon plates, 220 µm thick [80].

Stages of PV module production						
Component costs	**Charge material**	**Casting process**	**Plate cutting**	**Solar cell production**	**Module production**	**Total [€/W_p]**
Devices		0,03	0,03	0,09	0,07	0,22
Labour		0,03	0,05	0,11	0,17	0,36
Material	0,27	0,04	0,08	0,15	0,42	0,96
Loss		0,04	0,06	0,09	0,06	0,25
Additional		0,06	0,02	0,13	0,11	0,32
Total [€/W_p]	**0,27**	**0,20**	**0,24**	**0,57**	**0,83**	**2,11**

The dynamic progress in the research and technological work causes a systematic drop of the cell and module prices. Currently, it is possible to purchase a solar cell at the price of 1,2 \$/W_p and a module – at the price of 1,60 \$/W_p [81]. In this aspect, one should emphasize the fact that the big expectations concerning organic cells are mitigated by the preliminary calculations of the production costs for modules made of such cells, which, despite the low price of the organic base material, are estimated to be at the price level of silicon cell modules, yet with no guarantee of stability of the initial parameters at the time of operation.

The costs of the PV system will largely depend on the latter's established initial power, as well as the type and location of their installation. For small PV systems, the

costs of the photovoltaic modules constitute about 73 % of the costs of the whole system. Table 11 presents a proportional share of the costs of particular components of an integrated PV system, in the photovoltaics terminology referred to as the Balance of System (BOS).

Tab. 11. Proportional share of costs for particular components of a 5 kW_p PV system [82].

PV system component	Cost share of PV system
Photovoltaic modules	73 %
Supporting structure, installation	8 %
Conduits, junction boxes	3 %
Inverters	7 %
Project, documentation	6 %
Other	3 %

The relevance of the development of photovoltaics is also determined by the economic calculation, in which the basic importance is exhibited by the time of the refunding of the costs incurred for the PV system installation. This mainly depends on the purchase price of 1 W_p of power of the PV system and the price of 1 kWh of the electric energy produced by the PV system which is acquired by the producer. The cost refunding time will also be determined by the number of sun hours for a particular location, that is the time given in hours, during which a particular place is exposed to sun rays. In the case of Poland, this time is within the range of 1500 ÷ 1800 hours. In the economic calculation, one should also consider the interest rate, taking into account the credit cost or the deposit profit instead of the investment of the owned resources in the PV system installation. The calculation results for the refunding of the costs incurred for the purchase of a PV system, with the consideration of the above factors, are presented graphically in Figures 45 and 46.

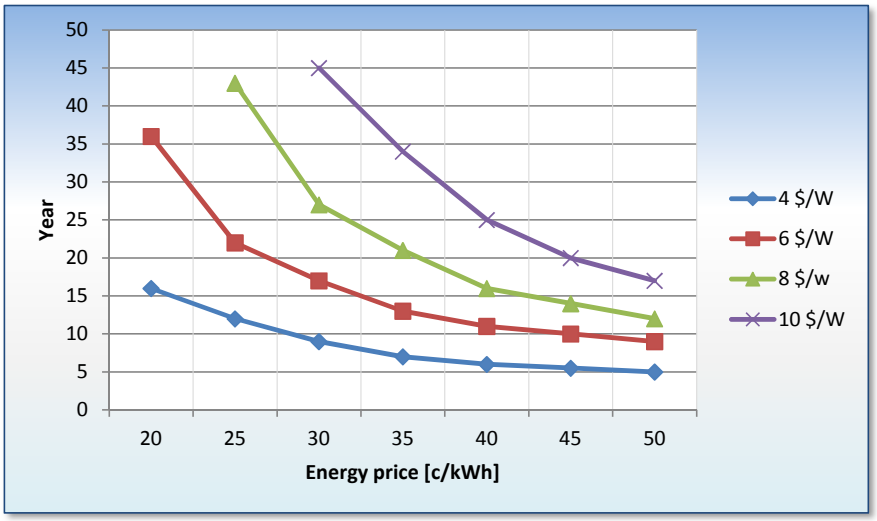

Fig. 45. Time of the refunding of the costs incurred for a PV system purchase, depending on the initial price of 1 W_p of the system power and the price of the electric energy produced by the system and treated as final product; calculations made with the assumption of a 5-hour system illumination and the interest rate of 5 % [7].

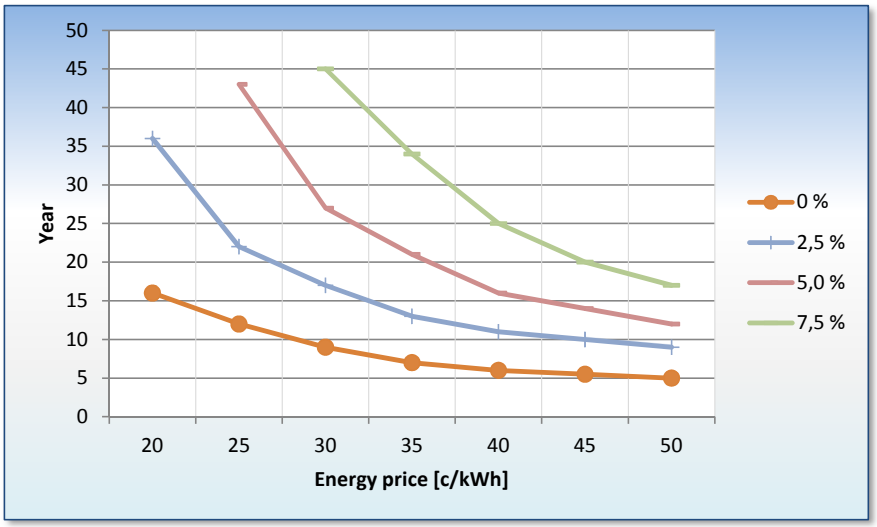

Fig. 46. Time of the refunding of the costs for a PV system depending on the market interest rate and the price of the electric energy produced by the system and treated as final product; calculations made with the assumption of a 5-hour system illumination and the price of the PV system installation equaling 8 $/1 W_p [7].

As it can be inferred from the dependences presented above, with the adequately low interest rate and with the price of the electric energy at the level of 20 cents per 1 kWh, the refunding of the costs incurred for the PV system installation

is due to be after 20 years of operation. According to the American reports, the cost of the "solar" electric energy depends on the size of the PV system and the insolation of the given location [7].

Tab. 12. Cost of the electric energy produced by a photovoltaic system on the basis of the American market's analysis [7].

Insolation	PV system type	PV system power	PV system price	Electric energy production cost
2000 kWh/m^2	Autonomous or integrated	2 kW$_p$	**15 022,00 $** - 7,5 $/W$_p$	31,63 c/kWh
1000 kWh/m^2				69,58 c/kWh
2000 kWh/m^2	Free-standing, integrated with network	50 kW$_p$	**274 213,00 $** - 5,5 $/W$_p$	21,90 c/kWh
1000 kWh/m^2				48,18 c/kWh
2000 kWh/m^2	BIPV (roof), integrated with network	500 kW$_p$	**1 990 330,00 $** - 4,0 $/W$_p$	16,91 c/kWh
1000 kWh/m^2				37,20 c/kWh

As it can be inferred from the data included in Table 12, the cost of the electric energy produced by a large photovoltaic power plant located in the intertropical area is only twice as high as the price of the conventional electric power. It is also a derivative of the costs of the PV system installation for 1 W$_p$ of its power, depending on the size and type of the system. According to this data, with the average annual insolation of about 1200 kWh/m^2 for the area of Poland, the costs of the electric energy produced by a PV system will be within the range of 1,1 ÷ 2,0 PLN /kWh, depending on the system's power.

One of the more important factors supporting the development of photovoltaics are the legal regulations concerning the price of the electric energy from renewable energy sources. In the case of the energy obtained from PV systems, this special tariff required for the network recipients who are simultaneously commercial energy distributors, is referred to as the feed-in tariff. It is currently effective in most European countries, and its value often depends on the power and type of the PV system.

Tab. 13. Value of the feed-in tariff in exemplary European countries [83].

Country	Type of PV system	System power	Feed-in tariff value
Switzerland	Free-standing	< 10 kW_p	0,39 €/kWh
		≥ 100 kW_p	0,30 €/kWh
	BIPV	< 10 kW_p	0,55 €/kWh
		≥ 100 kW_p	0,38 €/kWh
Bulgaria	Any	< 5 kW_p	0,44 €/kWh
		≥ 5 kW_p	0,41 €/kWh
The Czech Republic	Any	< 30 kW_p	0,46 €/kWh
		≥ 30 kW_p	0,45 €/kWh
Germany	BIPV	< 30 kW_p	0,33 €/kWh
		≥ 30 kW_p	0,31 €/kWh
		≥ 100 kW_p	0,29 €/kWh
		≥ 1 MW_p	0,24 €/kWh
	Free-standing	Any	0,24 €/kWh

With the current prices of electric energy, the development of photovoltaics significantly depends on the energy policy and the economic policy of the given country. All kinds of reports emphasize the fact that the price of the electric energy from conventional sources will not change its increasing tendency, and the price of the energy from unconventional sources will depend on the scientific and technological development, and within the period of ten years, these two energy prices will level. The currently incurred inputs will provide the given countries with a technological and economical supremacy in photovoltaics, which can be stated through the analysis of the development of this sector in Germany, the USA, China and Japan. Especially the pragmatic policy in China, financially and politically supporting the development of photovoltaics, has resulted in every second PV module in the world at the average price of 1,5 €/W_p to be currently produced in this country, and the development plans up to 2020 assume the installation of photovoltaic systems of the total power of 20 GW_p. Another example is Poland's neighbour, Germany, where the national policy together with the very high awareness and knowledge of the society bring positive effects in the development of the PV sector and its contribution to the economy. While in 2008, the magnitude of the German photovoltaic installations equaled 1,8 GW_p, in 2009, it reached the level of 3,5 GW_p [84].

7. Summary

To sum up the facts on photovoltaics discussed above, one should also consider the positive and negative aspects of the above method of electric energy production, from the point of view of the needs and the energy security of the modern civilization. The most important merits are the non-existing cost of power supply, the self-operating and long-term work, the possibility of decentralization of the energy generation process, as well as the difficulty in localizing the PV system, which is mostly significant in the moment of armed conflict. A negative evaluation can be supported by such aspects as the day's and year's periodicity of the PV system's effective operation, as well as the higher costs of the electric energy production as compared to those offered by the conventional power engineering, although one should expect the latter to cease to be valid within the next twenty years. Certain solutions provide the possibility to eliminate the problems connected with the day's periodicity of the PV system's work. One of them is assigning a part of the electric energy produced by the PV system to supply the process of electrolysis and hydrogen generation, which, at the time when the PV system is not illuminated, powers the fuel cell and provides the continuity in the electric energy supply through the hybrid PV system. The total power of the PV systems currently installed in the world equals about 69 GW_p [8] and it constitutes only less than 2 % of the total capacity of the world's existing conventional, wind, water and atomic power stations, which is estimated for about 3,5 TW. However, taking into account the dynamic growth of the photovoltaic cell production, which in 2011, exceeded 29 GW_p per year, one should expect a change in the above proportions in favour of the solar power engineering. Photovoltaics is, at present, an important element of the world's economy, and its progress, for many fundamental reasons, will, in the nearest future, be the motor for a further growth in the economy and the social level, and above all, in the energy security of the 21-nd century's societies.

Also in Poland, one can observe paramount perspectives for photovoltaics. The "feed-in tariffs" system proposed by the Ministry of Economy for the households open to the production of green energy, which is already being applied in most European countries, is based on four pillars:

1) Facilitation in the connection and operation of the Renewable Energy Source (RES) installations,
2) A clear and attractive system of extra payments for the sale of green energy produced in households,
3) A stable income perspective in the period of over a dozen years,

4) Periodical reviews of the tariff rates; effective, however only for the installations put to use after the introduction of the act.

In the last reports issued by the department of economy, the stable tariff rates mean that, due to the introduction of the FiT system, the owners of the RES household installations will be able to draw income from the energy they produce, which can be even a few times more than the price of its purchase. In the case of household photovoltaic installations, the owner of one which was put to use within the first two years after the introduction of the act, will receive 1100 PLN for 1 MWh of the produced current, for the period of 15 years.

References

[1] J. Bernreuter, "Nano-columns and Other Tricks", Sun&Wind Energy, 1, (2010), p. 100-105.
[2] P. J. Reddy, "Science and Technology of Photovoltaics", BS Publication, India, 2010.
[3] M. A. Green, K.. Emery, Y. Hishikawa, W. Warta, "Solar Cell Efficiency Tables", Progress in Photovoltaics: Research and Applications, 16, (2008), p. 435-440.
[4] D. Wortmann, "The Sun Rises Again Over Japan", PV Magazine, 2, (2008), p. 42-43.
[5] www.wholesalesolar.com
[6] J. Bernreuter,"After the Boom", Sun & Wind Energy, 7, (2010), p. 125-129.
[7] www.solarbuzz.com, www.irc.ec.europa.eu
[8] GLOBAL MARKET OUTLOOK FOR PHOTOVOLTAICS UNTIL 2016 – EPIA Report , EPIA, (2012), p. 5
[9] www.enf.cn
[10] S. Hausmann, „The Sun is Rising in the East", Sun&Wind Energy, 10, (2009), p. 90-103
[11] G. Hahn, P. Geiger, P. Fath, E. Bucher, „Hydrogen Passivation of Ribbon Silicon – Electronic Properties and Solar Cell Results",Proc. of the 28th IEEE Photovoltaic Specialistis Conference, 15-22 September 2000, Anchorage, p. 95-98.
[12] J. Bernreuter, "Good Thinks Come to Those Who Wait", Sun&Wind Energy, 11, (2010), p. 102-105.
[13] Information in "News", Photovoltaics International, 3, (2009), p. 10.
[14] Information in "The PV-Tech Blog", Photovoltaics International, 3, (2009), p. 208.
[15] K. W. Bőer, "Survey of Semiconductor Physics", Van Nostrand Reinhold, New York, 1992.
[16] A. Goetzberger, J. Knobloch, B. Voss, "Crystalline Silicon Solar Cell", John Wiley & Sons, Chichester, England, 1998.
[17] Z. M. Jarzębski, "Energia Słoneczna – Konwersja Fotowoltaiczna", PWN, Warszawa, 1990.
[18] J. I. Pankove, "Zjawiska Optyczne w Półprzewodnikach", WNT, Warszawa, 1974.
[19] P. A. Basore, "Numerical Modeling of Textured Silicon Solar Cells Using PC-1D", IEEE Trans. on Electron Devices, 37, (1990), p. 337-343.
[20] P. Menna, G. Di Francia, and V. La Ferrara, "Porous Silicon in Solar Cells: A Review and a Description of Its Application as an AR Coating", Solar Energy Mater. Solar Cells, 37, (1995), p. 13-24.
[21] B. M. Damiani, R. Lüdemann, D. S. Ruby, S. H. Zaidi, A. Rohatgi, "Development of RIE-textured Silicon Solar Cells", Proc. of the 28th IEEE Photovoltaic Specialistis Conference, 15-22 September 2000, Anchorage, p. 371-374.
[22] K. Shirasawa, H. Takahashi, Y. Inomata, K. Fukui, K. Okada, M. Takayama, H. Watanabe, "Large Area High Efficiency Multicrystalline Silicon Solar Cells", Proc. of the 12th European Photovoltaic Solar Energy Conference, vol. 1, 11-15 April 1994, Amsterdam, p. 757-760.
[23] J. Szlufcik, P. Fath, J. Nijs, R. Mertens, G. Willeke, E. Bucher, "Screen Printed Multicrystalline Silicon Solar Cells with a Mechanically Prepared V-Grooved Front Texturization", Proc. of the 12th European Photovoltaic Solar Energy Conference, vol. 1, 11-15 April 1994, Amsterdam, p. 769-772.
[24] P. Fath, G. Willeke, "Mechanical Wafer Engineering for High Efficiency Policrystalline Silicon Solar Cells", Proc. of the 12th European Photovoltaic Solar Energy Conference, vol. 1, 11-15 April 1994, Amsterdam, p. 1037-1040.
[25] L. Pirozzi, M. Garozzo, E. Salza, "The Laser Texturization in a Full Screen Printing Fabrication Process of Large Area Poly Silicon Solar Cells", Proc. of the 12th European Photovoltaic Solar Energy Conference, vol. 1, 11-15 April 1994, Amsterdam, p. 1025-1028.
[26] M. A. Green, S. R. Wenham, J. Zhao, "High Efficiency Silicon Solar Cells", Proc. of the 11th European Photovoltaic Solar Energy Conference, 12-16 October 1992, Montreux, p. 41-44.
[27] R. Lüdemann, B. M. Damiani, A. Rohatgi, "Novel Processing of Solar Cells with Porous Silicon Texturing", Proc. of the 28th IEEE Photovoltaic Specialistis Conference, 15-22 September 2000, Anchorage, p. 299-302.

[28] C. Lévy-Clément, S. Lust, S. Bastide, Q. N. Lê, Dominique Sarti, "Macropore Formation on P-type Multicrystalline Silicon and Solar Cells", Proc. of the 3rd International Conference Porous Semiconductors – Science and Technology, 10-15 March 2002, Puerto de la Cruz, p. 8-9.
[29] H. F. W. Dekkers, F. Duerinckx, J. Szlufcik, J. Nijs, "Silicon Surface Texturing by Reactive Ion Etching", Opto-electronics Rev., 8 (2000), p. 311-316.
[30] M. Lipiński, P. Panek, E. Bełtowska, V. Yerokhov, "Investigation of Macroporous Layer by Chemical Etching for Silicon Solar Cell Manufacturing", Proc. of the 17th European Photovoltaic Solar Energy Conference, 22-26 October 2001, Munich, p. 1786-1788.
[31] J. Zhao, A. Wang, M. Green, "19.8% Efficient Multicrystalline Silicon Solar Cells with Honeycomb Textured Front Surface", Proc. of the 2nd World Conference on Photovoltaic Solar Energy Conversion, 6-10 July 1998, Vienna, p. 1681-1684.
[32] M. J. Stocks, A. J. Carr, A. W. Blakers, "Texturing of Polycrystalline Silicon", Solar Energy Materials and Solar Cells, 40, (1996), p. 33-42.
[33] J. Szlufcik, F. Duerinckx, J. Horzel, E. van Kerschaver, R. Einhaus, K. De Clerco, H. Dekkers, J. Nijs, "Advanced Concepts of Industrial Technologies of Crystalline Silicon Solar Cells", Optoelectronics Rev., 8, (2000), p. 299-306.
[34] H. Nagel, A. G. Aberle, R. Hezel, "Optimised Antireflection Coatings for Planar Silicon Solar Cells Using Remote PECVD Silicon Nitride and Porous Silicon Dioxide", Progress in Photovoltaics: Research and Applications, 7, (1999), p. 245-260.
[35] C. Lévy-Clément,"Optical Properties of Porous Silicon Tuned by Electrochemical Reactions: Application to High Efficiency Solar Cells" in "Mass and Charge Transport in Inorganic Materials: Fundamentals and Devices", P. Vincenzini, V. Buscaglia, Techna Srl, 2000, p. 1311-1322.
[36] I. Lee, D. G. Lim, K. H. Kim, S. H. Kim, S. H. Lee, D. W. Kim, E. C. Choi, D. S. Kim, J. Yi, "Efficiency Improvement of Buried Contact Solar Cells Using MgF_2/CeO_2 Double Layer Antireflection Coatings", Proc. of the 28th IEEE Photovoltaic Specialistis Conference, 15-22 September 2000, Anchorage, p. 403-406.
[37] B. Lenkeit, T. Lauinger, A. G. Aberle, R. Hezel, "Comparison of Remote Versus Direct PECVD Silicon Nitride Passivation of Phosphorus-Diffused Emitters of Silicon Solar Cells", Proc. of the 2nd World Conf. and Exibition on Photovoltaic Solar Energy Conversion, 6-10 Juli, 1998, Vienna, p. 1434-1437.
[38] R. K. Pandey, L. S. Patit, J. P. Bange, D. K. Gautam, "Growth and Charakterization of Silicon Nitride Films for Optoelektronics Application", Optical Materials, 27, (2004), p. 139-146.
[39] S. R. Bryce, J. E. Cotter, C. B. Honsberg, S. R. Wenham, "Novel Uses of TiO_2 in Crystalline Silicon Solar Cells", Proc. of the 28th IEEE Photovoltaic Specialists Conference, 15-22 September, 2000, Anchorage, p. 375-378.
[40] J. E. Cotter, B. S. Richards, F. Ferraza, C. B. Honsberg, T. W. Leong, H. R. Mehrvarz, G. A. Naik, S. R. Wenham, "Design of a Simplified Emiter Structure for Buried Contact Solar Cells", Proc. of the 2nd World Conf. and Exibition on Photovoltaic Solar Energy Conversion, 6-10 Juli, 1998, Vienna, p. 1511-1514.
[41] B. C. Charkravarty, P. N. Vinod, S. N. Singh, B. R. Chakraborty, "Design and Simulation of Antireflection Coating for Application to Silicon Solar Cells", Solar Energy Mater. Solar Cells, 73, (2002), p. 56-66.
[42] R. Ahmad-Bitar, D. E. Arafah, "Processing Effects on the Structure of CdTe, CdS and SnO_2 Thin Films", Solar Energy Mater. Solar Cells, 51, (1998), p. 83-93.
[43] C. Beneking, W. A. Nositschka, O. Kluth, G. Schőpe, F. Birmans, H. Siekmann, B. Rech, "Application of Textured Zink Oxide Films to Obtain Black Multicrystalline Silicon Solar Cell", Proc. of the 16th European Photovoltaic Solar Energy Conference, 1-5 May, 2000, Glasgow, p. 1230-1233.
[44] E. G. Woelk, H. Kräutle, H. Beneking, "Measurement of Low resistive Ohmic Contacts on Semiconductors", IEEE Trans. on Electron Devices, ED-33, (1986), p. 19-22.

[45] M. M. Hilali, A. Rohatgi, B. To, "A Review and Understanding of Screen-Printed Contacts and Selective-Emitter Formation", Proc. of the 14th Workshop on Crystalline Silicon Solar Cells and Modules, 8-11 August, 2004, Winter Park, Colorado, p. 1-9.
[46] D. K. Schroder, "Liftime in Silicon", Solid State Phenomena, 6 &7, (1989), p. 383-394.
[47] T. Figielski, "Zjawiska Nierównowagowe w Półprzewodnikach", PWN, Warszawa, 1980.
[48] A. G. Aberle, "Surface Passivation of Crystalline Silicon Solar Cells: A Review", Progress in Photovoltaics: Research and Applications, 8, (2000), p. 473-487.
[49] M. J. Stocks, A. W. Blakers, "Theoretical Comparison of Conventional and Multilayer Thin Silicon Solar Cells", Progress in Photovoltaics: Research and Applications, 4, (1996), p. 34-54.
[50] J. D. Moschner, J. Henze, J. Schmidt, R. Hezel,"High-quality Surface Passivation of Silicon Solar Cell in an Industrial-type Inline Plasma Silicon Nitride Deposition System", Progress in Photovoltaics: Research and Applications, 12, (2004), p. 21-31.
[51] C. Hodson, E. Kessels, "Using ALD for Improved Efficiency Crystalline Silicon Solar Cells", Photovoltaics World, 4, (2009), p. 17-21.
[52] B. Sopori,"Silicon Nitride Processing for Control of Optical and Electronic Properties of Silicon Solar Cells", Journal of Electronic Materials, 32, (2003), p. 1034-1042.
[53] N. Arifuku, M. Dhamrin, M. Suda, T. Saitoh, K. Kamisako, "Passivation Effect of a-Si and SiNx: H Double Layer Deposited at Low Temperature Using RF-Remote PECVD Method'', Proc. of the 21st EPSEC, 4-8 September 2006, Dresden, p.877-880.
[54] N. A. Arora, J. R. Hauser, "Spectral Response of n^+-n-p and n^+-p Photodiodes", IEEE Trans. on Electron Devices, ED-34, (1984), p. 430-434.
[55] A. Tumański, Z. Sawicki, J. Oleński, J. Baniewicz, "Technologia Wytwarzania Półprzewodnikowych Złącz Dyfuzyjnych" w "Procesy Technologiczne w Elektronice Półprzewodnikowej", Wyd. Naukowo-Techniczne, Warszawa, 1973.
[56] S. Peters, H. Lavtenschlager, W. Warta, R Schindler, "RTP-Processed 17.5 % Efficient Silicon Solar Cells Featuring Record Small Thermal Budget", Proc. of the 16th European Photovoltaic Solar Energy Conf., 1-5 May, 2000, Glasgow, p. 1116-1119.
[57] M. Sasani, "The Simple Approach to Determination of Active Diffused Phosphorus Density in Silicon", Semiconductor Physics, Qantum Electronics & Optoelectronics, 7, (2004), p. 22-25.
[58] T. Żdanowicz, "Pomiary ogniw i modułów fotowoltaicznych", Wykłady i Komunikaty XII Szkoły Optoelektroniki "Fotowoltaika – ogniwa słoneczne i detektory podczerwieni", 22-24 maja 1997, Kazimierz Dolny, str. 159-172.
[59] N. Enebish, D. Agchbayar, S. Dorjkhand, D. Baatar, I. Ylemj,''Numerical Analysis of Solar Cell Current-Voltage Characterstics'', Solar Energy Mater. Solar Cells, 29, (1993), p. 201-208.
[60] M. Wolf, G. T. Noel, R. J. Strin, "Investigation of the Double Exponential in the Current-Voltage Characteristics of Silicon Solar Cells", IEEE Trans. on Electron Devices, ED-24, (1977), p. 419-428.
[61] www.solarlight.com
[62] W. Shockley, H. J. Queisser, "Detailed Balance Limit on Efficiency of P-N Junction Solar Cells", J. Appl. Phys. 8, (1961), p. 510-519.
[63] T. Tiedje, E. Yablonovitch, G. Cody, B. G. Brooks, "Limiting Efficiency of Silicon Solar Cells", IEEE Trans. on Electron Dev., vol. ED-31, no. 5, (1984), p. 711-716.
[64] M. A. Green, K. Emery, D. L. King, S. Igari, W. Warta, "Solar Cell Efficiency Tables (Version 23)", Progress in Photovoltaics: Research and Applications, 12, (2004), p. 55-62.
[65] S. R. Wenham, C. B. Honsberg, S. Edmiston, L. Koschier, A. Fung, M. A. Green, F. Ferrazza, "Simplified Burid Contact Solar Cell Process", Proc. of the 25th IEEE Photovoltaic Specialists Conf. 13-17 May 1996, Washington, p. 389-392.
[66] M. Taguchi, K. Kawamoto, S. Tsuge, T. Baba, H. Sakata, M. Morizane, K. Uchihashi, N. Nakamura, S. Kiyama, O. Oota, "HIT™ Cells – High Efficiency Crystalline Si Cells witz Novel Structure", Progress in Photovoltaics: Research and Applications, 8, (2000), p. 503-513.
[67] H. Sakata, T. Nakai, T. Baba, M. Taguchi, S. Tsuge, K. Uchihashi, S. Kiyama, "20.7 % Highest Efficiency Large Area (100.5 cm^2) HIT™ Cell", Proc. of the 28th IEEE Photovoltaic Specialistis Conference, 15-22 September 2000, Anchorage, p. 7-12.

[68] E. Schneiderlöchner, G. Emanuel, G. Grupp, H. Lautenschlager, A. Leimenstoll, S. W. Glunz, R. Preu, G. Willeke, ''Silicon Solar Cells with Screen Printed-Front Contact and Dielectrically Passivated, Laser-Fired Rear Electrode'', Proc., of the 19th Europ. PSEC, 7-11 June 2004, Paris, p.447-450.
[69] E. van Kerschaver, G. Beaucarne, "Back-contact Solar Cells: A Review", Progress in Photovoltaics: Research and Applications, 14, (2006), p. 107-123.
[70] J. Poortmans, V. Arkhipov, "Thin Film Solar Cells – Fabrication, Characterization and Applications", John Wiley & Sons, Chichester, England, 2006.
[71] E. Fortunato, D. Ginley, H. Hosono, D. C. Paine, "Transparent Conducting Oxides for Photovoltaics", MRS Bulletin, 32, (2007), p. 242-247.
[72] S. Niki, M. Contreras, I. Repins, M. Powalla, K. Kushiya, S. Ishizuka, K. Matsubara, "CIGS Absorbers and Processes", Progress in Photovoltaics: Research and Applications, 18, (2010), p. 453-466.
[73] P. Grunow, S. Lust, D. Sauter, V. Hoffmann, C. Beneking, B. Litzenburger, L. Podlowski, "Weak Light Performance and Annual Yields of PV Modules and Systems as a Result of the Basic Parameter Set of Industrial Solar Cells", Proc. of the 19th European Photovoltaic Solar Energy Conference, 7-11 June, 2004, Paris, p. 2190-2193.
[74] www.pvresources.com
[75] H. Kaan, T. Reijenga, "Photovoltaics in an Architectural Context", Progress in Photovoltaics: Research and Applications, 12, (2004), p. 395-408.
[76] www.sunways.de
[77] www.voltwerk.com
[78] News in "Products Information", Sun & Wind Energy, 7, (2010), p. 157.
[79] E. Klugmann-Radziemska, "Fotowoltaika w teorii i praktyce", BTC, Legionowo 2010.
[80] C. del Cañizo, G. del Coso, W. C. Sinke, "Crystalline Silicon Solar Module Technology", Progress in Photovoltaics: Research and Applications, 17, (2009), p. 199-209.
[81] www.pvinsights.com
[82] M. Bächler, "Thin Future – Outlook for Grid-Connected PV Systems in Europe", Renewable Energy World, 4, (2006), p. 150-161.
[83] www.solarfeedintariff.net
[84] S. Tetzlaff, "We All Hope that Grid Parity Will Come Soon", Sun&Wind Energy, 4, (2010), p. 168-169.
[85] F. Granek, high-efficiency back-contact back-junction silicon solar cell, Dissertation, Fraunhofer Institut für Solare Energiesysteme (ISE) 2009, p. 45-48.
[86] D. De Ceuster, P. Cousins, D. Rose, D. Vicente, P. Tipones, and W. Mulligan, Low Cost, high volume production of >22% efficiency silicon solar cells, in Proceedings of the 22nd European Photovoltaic Solar Energy Conference, Milan, Italy, (2007), p.816-9.